Transformation of inherent microorganisms in Wyoming-type bentonite and their effects on structural iron

Miettinen, Hanna

2022-05

Miettinen , H , Bomberg , M , Bes , R , Tiljander , M & Vikman , M 2022 , ' Transformation of inherent microorganisms in Wyoming-type bentonite and their effects on structural iron ' , Applied Clay Science , vol. 221 , 106465 . https://doi.org/10.1016/j.clay.2022.106465

http://hdl.handle.net/10138/343726
https://doi.org/10.1016/j.clay.2022.106465

Applied Clay Science 221 (2022) 106465

Contents lists available at ScienceDirect

Applied Clay Science

journal homepage: www.elsevier.com/locate/clay

Transformation of inherent microorganisms in Wyoming-type bentonite and their effects on structural iron

Hanna Miettinen [a,*], Malin Bomberg [a], René Bes [b,c], Mia Tiljander [d], Minna Vikman [a]

[a] VTT Technical Research Centre of Finland Ltd., Tietotie 2, Espoo, P.O.Box 1000, FI-02044 VTT, Finland
[b] Department of Physics, University of Helsinki, P.O. Box 64, FI-00014 Helsinki, Finland
[c] Helsinki Institute of Physics, P.O. Box 64, FI-00014 Helsinki, Finland
[d] Geological Survey of Finland, Vuorimiehentie 2K, FIN-02150 Espoo, Finland

ARTICLE INFO

Keywords:
Sulfate reduction
Iron reduction
Bentonite structural iron
Microbiome

ABSTRACT

Bentonite is one of the materials used to construct engineered barriers in high-level radioactive nuclear waste geological disposal with its many advantageous features such as low hydraulic conductivity, self-sealing ability, durability, adsorption and immobilization of metals and radionuclides and reduction of microbial activity. Many of these properties are linked with the bentonite swelling capability. Transformations of indigenous microorganism communities from Wyoming-type bentonite and the Finnish repository site groundwater and their effects on the bentonite structural iron over five years were studied in repository relevant anoxic and oxic slurry conditions. Active sulfate reduction (0.06 nmol mL^{-1} day^{-1}) was detected in the anoxic microcosm waters after a year, however after two years sulfate reduction was not active anymore. Microbial numbers determined by quantitative PCR in the bentonite slurry of both experiment types supported the finding of decrease of overall microbial activity after a year of incubation that was not maintained anymore by the dissolving organic carbon from the bentonite. Regular electron donor additions (final concentration of 2 mM for formate and acetate each, three times per year) activated the microbiome resulting in increasing numbers of bacterial 16S rRNA gene copies and sulfate reducers (*dsr*B gene copies) as well as detection of sulfide in the water phase of both experiment types. After 4.9 years the structural iron in the fine portion of the montmorillonite had become completely reduced in all microbial microcosms and minor smectite illitization was detected especially in anoxic microcosms. Dominating bacterial groups at the end of the experiment were mainly known sulfur/sulfate and iron reducers. Archaea and fungi constituted a minor part of the microbiomes. In originally oxic microcosms, the bacterial 16S RNA and *dsr*B gene copy numbers were lower than in the anoxic experiment but started to significantly increase after the electron donor additions. Microorganisms originating from the repository environment could reduce the bentonite structural iron in a few years to an extent likely to affect the bentonite swelling ability if sufficient amounts of suitable electron donors are available in localized areas where bentonite is not at high density and pressure in the geological disposal.

1. Introduction

Disposal of high-level radioactive nuclear waste into deep underground geological repository is a globally considered solution (Lloyd and Cherkouk, 2020; Sellin and Leupin, 2013; OECD, 2000). Geological disposal comprises an engineered multibarrier concept that includes a waste container, an engineered barrier, and the final geological barrier. In Finland the disposal of the nuclear waste into a geological repository has been planned to start already during 2020s. The Finnish concept consists of copper/iron waste canisters disposed in deposition holes drilled at around 400 m below the ground surface in originally anoxic crystalline bedrock, buffer bentonite to surround the canisters and backfill to line and seal the holes and tunnels of the repository. The disposal concept has mainly been planned considering the abiotic interactions within the canisters, sealant and bedrock, affecting the long-term safety of the system. However, during recent years a lot of research has shown that the microbial activity is a relevant factor in the system regarding to the bedrock (Bomberg et al., 2016; Bomberg et al., 2015; Sohlberg et al., 2015), bentonite (Maanoja et al., 2020; Grigoryan et al., 2018; Masurat et al., 2010) and canisters (Carpén et al., 2018; Rajala

* Corresponding author.
E-mail address: hanna.miettinen@vtt.fi (H. Miettinen).

https://doi.org/10.1016/j.clay.2022.106465
Received 10 September 2021; Received in revised form 16 February 2022; Accepted 22 February 2022
Available online 11 March 2022

et al., 2015; Pedersen, 2010).

The role of bentonite in nuclear waste geological disposal is to protect the waste canisters and to seal off the disposal galleries from the shafts that lead to the surface (Sellin and Leupin, 2013). The main requirements for buffer material are low hydraulic conductivity to limit water movement, self-sealing ability to fill engineering gaps and extremely long-term durability properties (Sellin and Leupin, 2013). In addition, properties such as adsorbing and immobilizing selective metals and radionuclides (Dong, 2012; Pusch et al., 2012), ability to reduce microbial activity (Bengtsson and Pedersen, 2017) and low gas permeability are beneficial features. Microbial activity in bentonite is restricted only in water saturated high density conditions (Bengtsson and Pedersen, 2017). The loss of bentonite swelling capability even locally could have detrimental effects on the functionality and protective magnitude of the bentonite barrier in such location.

When bentonite has reached the final swelling pressure at the planned density, microbial activity is negligible (Bengtsson and Pedersen, 2017; Stroes-Gascoyne et al., 2011) as well as the movement of water and gas is minor. However, there can be areas in the repository, where bentonite density remains lower than planned, or water movement from water-carrying fracture host rock at the buffer interface can cause erosion (Stroes-Gascoyne et al., 2011). This can create localized points, where microorganisms are active for extended times. It has been suggested that microbial activity can affect bentonite by reducing sulfate to sulfide which abiotically reduces ferric iron to ferrous iron in bentonite (Pedersen et al., 2017) or directly by iron reduction by iron reducing bacteria (IRB). Some studies, in conditions supporting microbial activity, have even indicated the possibility of smectite illitization (Kim et al., 2004; Liu et al., 2012) that may result in notable changes in bentonite properties. The aim of this study was to examine in repository relevant anoxic and oxic slurry conditions that enable microbial activity the change over time in the structure of the indigenous bentonite and repository groundwater microbial communities and their effects on the bentonite.

2. Materials and methods

2.1. Materials

2.1.1. Bentonite

Bentonite used in experiments was room dry (91.5% dry matter content) Wyoming-type bentonite (American Colloid Company, USA) characterized earlier by Kiviranta and Kumpulainen (2011). The mineral composition of the bentonite, was studied semiquantitatively with FE-SEM-EDS (Table 1). Well polished epoxy mount was prepared from the bentonite material that composed mainly of montmorillonite (92.2%), K-feldspar (2.7%), plagioclase (1.8%), quartz (1.3%) and calcite (1.0%). The cation exchange capacity (CEC) of the bentonite before the experiment was 0.85 meq g^{-1} (milliequivalents g^{-1}; Table S1).

Table 1
Mineral composition of the used Wyoming-type bentonite and crushed rock studied with FE-SEM EDS analysis.

Minerals	Bentonite (%)	Minerals	Crushed rock (%)
Montmorillonite	92.2	Quartz	31.3
K-feldspar	2.7	Plagioclase	22.5
Plagioclase	1.8	Pyrrhotite	17.6
Quartz	1.3	Graphite	10.9
Calcite	1.0	Biotite	9.7
Sulfides	0.4	Muscovite	3.9
Biotite	0.2	Apatite	1.0
Siderite	0.2	Chlorite	0.9
Illite	0.1	K-feldspar	0.6
Apatite	0.1	Rutile	0.5
Fe silicate	<0.1	Garnet	0.3
Ilmenite	<0.1	Altered Fe-oxid	0.3
Baryte	<0.1	Fluorite	0.1
Hornblende	<0.1	Tourmaline	0.1
Muscovite	<0.1	Ilmenite	0.1
Zircon	<0.1	Pyrite	0.1
Gypsum	<0.1	Chalcopyrite	0.1
Kaolinite	<0.1		
Celestine	<0.1		

2.1.2. Rock

The rock material used in experiments was graphite-containing rock originating from Olkiluoto, the selected final disposal site of nuclear waste in Finland. The crushed rock contained mainly quartz (31.3%), plagioclase (22.5%), pyrrhotite (17.6%), graphite (10.9%), biotite (9.7%) and muscovite (3.9%) (Table 1) studied with FE-SEM-EDS from polished epoxy mounts.

2.2. Experimental set-up

Microcosms were set-up in sterile 100 mL headspace bottles, containing 5 g of room dry bentonite, 80 mL of water mixture and 5 g of crushed (2 to 5.6 mm) rock. The graphite containing crushed rock was added to support the endogenic chemotrophic microbial communities. Experiments were started from anoxic and oxic conditions to simulate the closure phase of the repository but also the later phase when oxygen has been consumed. For the anoxic microcosms, the dry bentonite was kept in open bottles in an anoxic glove box (N_2:CO_2:H_2 80:10:10) for at least 21 days with occasional mixing to remove oxygen from bentonite. The water mixture used in the anoxic experiment consisted of three deep groundwaters (drillholes OL-KR11, OL-KR13, ONK-KR15; 25 mL each) from Olkiluoto and a small portion (5 mL) of autoclaved and nitrogen (N_2) purged surface water from Korvensuo pool, Olkiluoto. The use of groundwater mixture ensured existence of diverse microbial communities and the surface water addition assisted in providing needed nutrients. In the oxic experiment the water mixture consisted mainly of the untreated Korvensuo pool water (65 mL) and the anaerobic groundwater mixture (15 mL). The added water mixtures contained approximately 6 mgL^{-1} DOC (Table S2) and the DIC values were lower in the oxic water (5 mgL^{-1}) than in the anoxic water (13 mgL^{-1}). Both water mixtures contained sulfate (57 and 120 mgL^{-1}, respectively for oxic and anoxic waters), whereas only the anoxic water contained sulfide (1.1 mgL^{-1}). Nitrogen, nitrate, nitrite, ammonium-nitrogen, phosphorus and phosphate levels were low and mainly below detection. Concentrations of metals and especially cations related to salinity such as calcium, sodium and magnesium were many times higher in the anoxic than in the oxic water mixture.

The microcosms were supplemented with a small amount of non-fermentable short chain organic electron donors so that the final concentrations were 0.1 mM for sodium acetate and sodium formate and 0.05 mM for methanol. The anoxic experiment microcosm bottles were closed in the anoxic glove box with sterile butyl rubber septa and aluminum crimp caps and the oxic microcosms were closed similarly in air in a laminar flow hood. The anoxic microcosms were supplemented with 15 mL of sterile filtered (0.22 μm) methane with a sterile syringe and needle through the rubber septum after the closure as methane is abundant in the Olkiluoto deep subsurface. Both experiment types included in addition to the microbial microcosms, so called bentonite microcosms, where the microorganisms were intended to originate mainly from the bentonite as the added waters were sterile filtered (0.22 μm). No additional electron donors were included in these bentonite microcosms. In addition, abiotic controls, with treatments to reduce the number of microbial cells and activity were included in both experiment types. In abiotic microcosms, bentonite was heat treated (180 °C, 16 h), water mixtures were sterile filtered and crushed rock was autoclaved (121 °C, 15 min), electron donors were also included. Anoxic microcosms were incubated at 30 °C and oxic microcosms at 37 °C in the dark. Compilation of the experiment is presented in the Table 2 and example image of microcosms is shown in Fig. 1. Two years and eight months

Table 2
Experimental set-ups in anoxic and oxic conditions.

Anoxic microcosm type	Components	Amount	Oxic microcosm type	Components	Amount
Microbiological	Wyoming-type bentonite	5 g	Microbiological	Wyoming-type bentonite	5 g
	Groundwater mixture	75 mL		Oxic surface water	65 mL
	Surface water	5 mL		Groundwater mixture	15 mL
	Crushed rock	5 g		Crushed rock	5 g
	Electron donors			Electron donors	
	Anoxic gas mixture			Air	
Bentonite	Wyoming-type bentonite	5 g	Bentonite	Wyoming-type bentonite	5 g
	Sterile filtered groundwater mixture	75 mL		Sterile filtered oxic surface water	65 mL
	Sterile filtered surface water	5 mL		Sterile filtered groundwater mixture	15 mL
	Crushed rock	5 g		Crushed rock	5 g
	No electron donors			No electron donors	
	Anoxic gas mixture			Air	
Abiotic	Heat treated Wyoming-type bentonite	5 g	Abiotic	Heat treated Wyoming-type bentonite	5 g
	Sterile filtered groundwater mixture	75 mL		Sterile filtered oxic surface water	65 mL
	Sterile filtered surface water	5 mL		Sterile filtered groundwater mixture	15 mL
	Autoclaved crushed rock	5 g		Autoclaved crushed rock	5 g
	Electron donors			Electron donors	
	Anoxic gas mixture			Air	

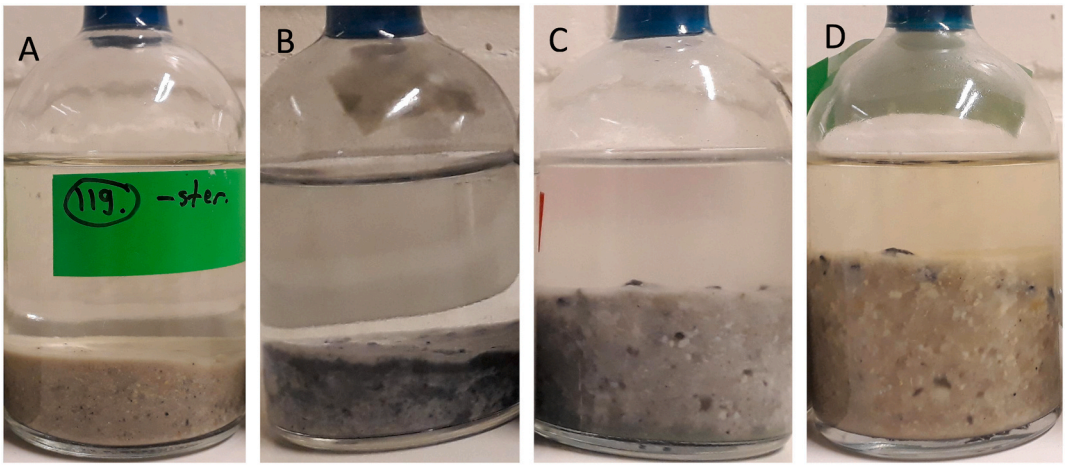

Fig. 1. Bentonite microcosms during the fourth year of the experiment. A) Anoxic abiotic control, B) Anoxic bentonite C) Oxic microbial and D) Oxic abiotic microcosms.

after incubation start all the remaining microcosms that were not yet studied were supplemented every fourth month with electron donors Na-acetate and Na-formate with final concentration of 2 mM each. This concentration was still low but higher than generally found in the oligotrophic Olkiluoto groundwaters where electron donors are efficiently utilized and accumulate only seldomly. All microcosms were studied at two weeks, one, two and 3.9 years (referred as 4 years) after the start of the experiments and additionally inspected time to time and photographed if visual changes were discovered. Additional bentonite samples for iron speciation measurements with XANES (X-ray absorption near edge structure) and for smectite-to-illite interactions with X-ray diffraction (XRD) were taken 4 years and 10 months after start of the experiment.

2.3. Methods

2.3.1. Gas phase composition and liquid phase chemistry

The headspace gas composition of the microcosms was measured with gas chromatography and the liquid phase chemistry of the used water mixtures for dissolved organic carbon (DOC), dissolved inorganic carbon (DIC), sulfate, sulfide, nitrogen, nitrate, nitrite, ammonium-nitrogen, phosphorus, phosphate, aluminum, potassium, calcium, copper, magnesium, manganese, sodium, silicon, iron, ferrous iron and total sulfur as well as the microcosms water phase for DOC, acetic and formic acid, sulfate, sulfide, total iron, pH, redox and conductivity were analyzed as described in the supplements.

2.3.2. Bentonite and crushed rock characterization

The modal mineralogy was determined from the original unpurified bentonite material used in the experiment. The mineralogy of the crushed rock and bentonite used in experiments was analyzed with Field emission scanning electron microscope (JEOLJSM 7100F Schottky) with energy dispersive spectroscopy EDS (Oxford Instruments X-Max SDD 80 mm^2) controlled by INCA Feature software. To identify the modal mineralogical composition over 25,000 points from bentonite and over 35,000 points from crushed rock particles was analyzed using grid-analysis. Seven areas were selected to measure crushed rock particles and all unidentified areas were classified as graphite. Bentonite cation exchange capacity was analyzed with the Cu-Trien method (Meier and Kahr, 1999; Amman et al., 2005). Bentonite samples at 4 years 10 months time point from each experiment and microcosm type from duplicate microcosms were anoxicly purified (size fraction <0.2 μm) and ion saturated (K, Mg) for XRD to identify smectite illite interaction between samples and for XANES measurements used for iron speciation measurements. Purification and XANES measurement protocols are described in detail in the supplements.

2.3.3. X-ray diffraction

Samples were analyzed using Bruker D8 Discover A25 diffractometer. Anod material was Cu (K-alpha 1 = 1.54060, K-Alpha 2 = 1.54439 (K-alpha mean = 1.4318), K-beta = 1.39222). Adjustment of the generator was 40 kV/40 mA, and spinner was used to improve the statistics. Samples were prepared from moist experiment samples sealed in anoxic environment. Bulk sample was made drying subsample under a fume hood overnight and fastening it on the glass slide using acetone. To study the clay mineralogy more closely a slurry was made by stirring moist bentonite to deionized water. A slurry sample was made pipetting slurry on the glass slide. The rest of the slurry was divided on two test tubes for ion exchange. 1 mL 0.1 M $MgCl_2$ and 1 mL 1 M KCl was added to separate test tubes, stirred and sealed overnight. Samples were washed 7 times with deionized water centrifuging in between to remove extra salts. Mg and K saturated samples were made pipetting slurry on glass slides. All pipetted samples were dried in room temperature under fume hood overnight. Mg saturated sample was treated with ethylene glycol (EG) at 60 °C > 16 h (Moore and Reynolds, 1997) and K saturated sample was heated 1 h at 200 °C and further 1 h at 550 °C. Bulk and slurry samples were measured over the range 2–70°2Theta, step size 0.02° with measurement time 0.1 s. Qualitative phase identification was done using Bruker EVA5.2 software and ICDD PDF-4 Minerals 2021 database (Fig. S1). Ion exchanged sample measurements were repeated after each treatment 2–35°2Theta, step size 0.02° and measurement time 0.2 s.

2.3.4. Sulfate reduction rate

Biological sulfate reduction rate (SRR) was measured in the water phase of the microcosm after the first and the second year with labeled $^{35}SO_4$ described in detail in the supplement.

2.3.5. DNA extraction

DNA was extracted from the original water mixtures used for the microcosms for anoxic and oxic experiments. Triplicate water samples from oxic (720, 750 and 770 mL) and anoxic (1500, 1550 and 1950 mL) experiments were filtered on nitrocellulose acetate filters (0.2 μm pore size, Corning, USA) by vacuum suction. DNA was extracted from the filters as described in Miettinen et al. (2019). Duplicate wet bentonite samples (10 mL) from the microcosms were extracted for DNA with a method modified from Lever et al. (2015) and described in the supplements. DNA from the dry original bentonite was also extracted from triplicate samples. The DNA concentration of all samples was determined using the Qubit 2.0 fluorometer (Thermo Fischer Scientific, USA).

2.3.6. Quantitative PCR

qPCR was applied to estimate the number of bacteria (16S rRNA gene), archaea (16S rRNA gene), fungi (5.8S rRNA gene) and sulfate reducers (*dsr*B gene) in the microcosms and in the used water mixtures. The abundance of bacterial and archaeal 16S rRNA gene copies and fungal 5.8S rRNA gene copies was determined by qPCR as described in Miettinen et al. (2021) and Bomberg and Miettinen (2020). The number of *dsr*B gene copies was estimated using the primer pair DSRp2060f and DSR4r (Wagner et al., 1998; Geets et al., 2006). The qPCR was performed using the SensiFAST Sybr No-ROX kit (Bioline, Meridian Biosciences, USA). The reactions contained 800 nM of primers and the amplification reactions consisted of denaturation step at 95 °C for 15 min, 45 cycles of 10 s at 95 °C, 35 s at 56 °C, 30 s at 72 °C, and final extension step for 3 min at 72 °C and a melting curve analysis.

All the bacterial, archaeal, fungal and *dsr*B amplifications were performed in triplicate using 10 μL reaction volumes and 1 μL of template DNA and run on the LightCycler 480 instrument (Roche Applied Science, Germany). Negative controls without added DNA template were included in each run. The bacterial, archaeal, fungal and *dsrB* gene amplification results were compared to that of a plasmid standard dilution series containing the 16S rRNA gene insert of *Escherichia coli* or *Halobacterium salinarum*, for bacteria and archaea, respectively, or the 5.8S rRNA gene of *Aspergillus versicolor* for fungi or the *dsr*B gene insert of *Desulfobacterium autotrophicum* for the *dsr*B quantification. Inhibition of the qPCR assays was found, and all samples were run using the 1/10 dilution to minimize the inhibition.

2.3.7. Amplicon sequencing

The bacterial, archaeal and fungal amplicon libraries were produced as in Miettinen et al. (2021) except for 5% dimethylsulfoxide used in PCRs. Libraries were sent for sequencing on the Ion Torrent PGM platform at Bioser (Biocenter Oulu Sequencing Center, Oulu, Finland). For samples, from which only a small number of bacterial, archaeal or fungal gene sequence reads were obtained, new amplicon libraries were prepared and sequenced. The sequence reads were analyzed using the Mothur software (v.1.43.0) (Schloss et al., 2009) as described in Miettinen et al. (2021) using the Silva database version 138 (Pruesse et al., 2007: Quast et al., 2013) and unmodified UNITE ITS database (version 8.2) (Kõljalg et al., 2013; Nilsson et al., 2019) for the fungal ITS sequences. Further analysis of the sequence data, visualization and statistical analysis are described in the supplements. The sequences have been submitted to the European Nucleotide Archive (http://www.ebi.ac.uk/ena) under study accession number PRJEB48658.

3. Results

3.1. Gas phase changes

The gas composition in the anoxic microcosms was relatively stable over time except for the first days and weeks (Fig. 2A). Hydrogen gas was detectable only from the abiotic control microcosms at the two-week measurement and disappeared by the fourth month also from these microcosms indicating that it had been used up by the microorganisms. In the microcosms that were closed in air (Fig. 2B) there was a clear decrease in the oxygen content during the first months in all microcosm types. The oxygen level decrease was the slowest in the abiotic microcosms as there was still around 5% oxygen left in the seventh month measurement, whereas in the microbial and bentonite microcosms the oxygen percentage was half of that. The oxygen level steadily decreased over the whole incubation time but slowly after the first year. After four years the oxygen level had decreased to approximately 1.5% in all oxic microcosms, whereas the oxygen level was below 0.5% in all anoxic microcosms at all times. This low oxygen level was likely an unavoidable contamination introduced during measurement. In the oxic microbial and bentonite microcosms the carbon dioxide percentage increased to over 7% in the fourth year from less than 0.3% in the second year. The individuality of the microcosms was noticed as one of the triplicate microbial microcosms had lower carbon dioxide level (3.9%) than the two others (8.6 and 8.7%).

3.2. Physico-chemical changes of the microcosms

Visual changes occurred in the bentonites during the incubation. A thin black layer developed on the surface of the bentonites in the anoxic microbial microcosms ten days after the start of the experiment (Fig. S2) and disappeared after a few months. At the end of the second-year brownish color was visible in most anoxic microcosms including a few abiotic microcosms (Fig. S3) which disappeared after a further half-year incubation. Within two weeks after the first addition of electron donors (32 months), the anoxic microbial (Fig. S4) and bentonite (Fig. S5) microcosms had a black precipitate on the bentonite-water interface. The black color strengthened and extended for several months until stabilizing or even decreasing at the end of the experiment. In the oxic microbial and bentonite microcosms black precipitate appeared around two months after the first electron donor addition and with lower intensity than in the anoxic microcosms and it was not detected in all bentonite microcosms (Fig. S6 and S7). At the last sampling (4 years) the bentonite color was grey with a green hue. No black precipitate was

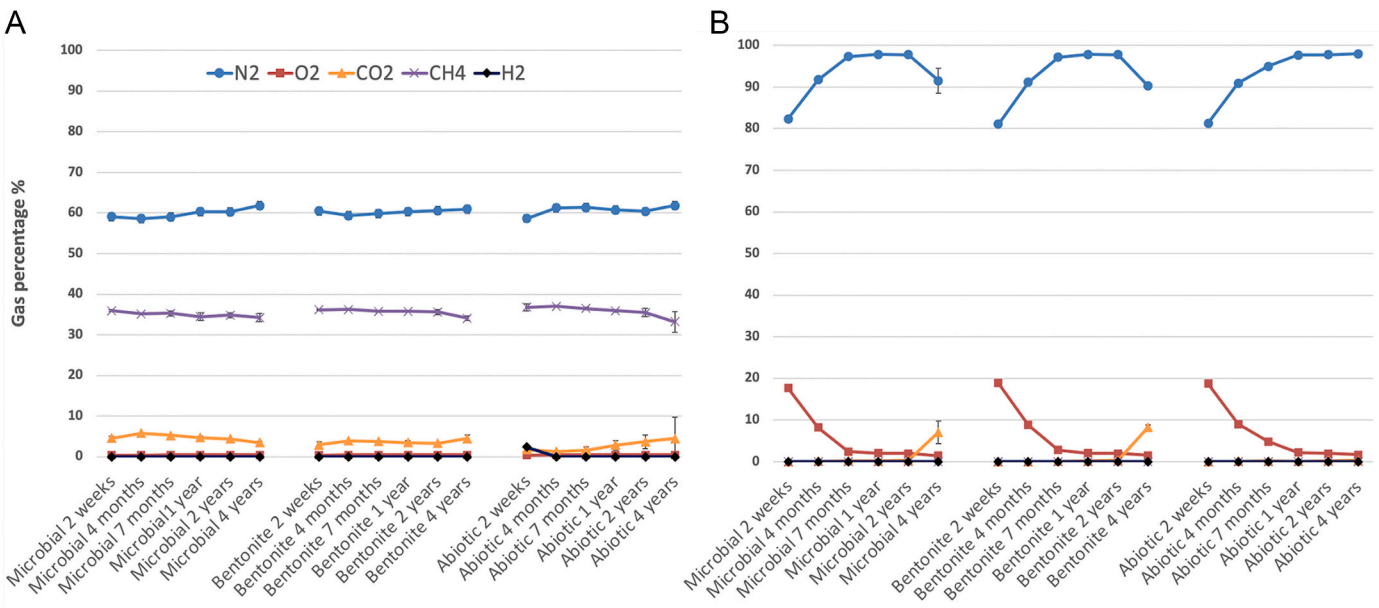

Fig. 2. The gas phase of A) the anoxic and B) the oxic bentonite experiment over four years.

observed in the abiotic anoxic or oxic microcosms during the study time (Figs. S8 and S9), however after 4 years and 10 months in some anoxic abiotic microcosms clear black coloring was visible (Fig. S10). There were prominent visual differences between replicates both in microbial and bentonite microcosms.

The cation exchange capacity (CEC) of the Wyoming-type bentonite before the experiment was 0.85 meq g^{-1} (milliequivalents g^{-1}; Table S1). After the first year the CEC values increased in the microbial and bentonite microcosms to 0.89 and 0.87 meq g^{-1}, respectively, whereas in the oxic microcosms the values were still low (0.84 meq g^{-1}). In the second year also the anoxic abiotic and oxic bentonite microcosms showed increased CEC values (0.88–0.89 meq g^{-1}), whereas after the fourth year all except the both abiotic microcosm types the CEC values had increased (0.88–0.93 meq g^{-1}; limit of error 0.017 meq g^{-1} with 95% confidence level).

pH of the water phase in the microcosms increased at first and then decreased being highest in the second-year measurements in all microcosm types (Table 3). pH was higher in the oxic experiment than in anoxic microcosms varying mostly above pH 8. Redox values were relatively high up to around 330 mV vs. SHE in the oxic microbial and bentonite microcosms and decreased down to 83 to 95 mV vs. SHE in the last year. The redox values in anoxic microbial and bentonite microcosms were the highest at the two-year time point, with the lowest redox values of −95 mV vs. SHE at the end of the experiment. Generally, the redox values in the abiotic microcosms were higher than in the microbial microcosms. The sulfate concentration in the water phase was increased already after two weeks in both experiment type microcosms (282 and 309 mg L^{-1}) compared to original water mixtures (57 and 120 mg L^{-1}) and the concentration further increased in both abiotic microcosm types as a function of time. However, in the anoxic microbial microcosms the sulfate concentration decreased in the first-year measurement to less than half of that found in the anoxic abiotic microcosms which indicates microbial sulfate reduction. A significant decrease in sulfate concentrations was detected in all microbial type microcosms in the fourth year as the sulfate concentrations were below the detection limit (<40 mg L^{-1}). No sulfide was detected in any of the second-year microcosms.

Table 3
pH, Redox, conductivity and concentration of sulfate, sulfide and total iron in the water phase of the bentonite microcosms over four years.

Experiment type	Microcosm type and sampling time	pH	Redox mV vs. SHE	Conductivity mS m^{-1}	Sulfate mg L^{-1}	Sulfide mg L^{-1}	Total iron mg L^{-1}
Anoxic	Two weeks				309		87
	Microbial 1 y	8.0	150.5	12.4	138		260
	Microbial 2 y	8.3	189.0	6.3*	232	< 0.1	66
	Microbial 4 y	7.8	−90.2	11.5	< 40	0.49	< 1000
	Bentonite 1 y	8.0	209.9	12.3	237		< 50
	Bentonite 2 y	8.5	238.3	6.3*	247	< 0.1	68
	Bentonite 4 y	7.7	−95.2	11.3	< 40	0.55	< 1000
	Abiotic 1 y	8.2	356.9	12.5	291		120
	Abiotic 2 y	8.5	184.8	6.4*	327	< 0.1	27
	Abiotic 4 y	7.3	217.2	11.7	348	< 0.1	< 1000
Oxic	Two weeks				282		< 50
	Microbial 1 y	8.6	330.0	3.7	334		150
	Microbial 2 y	8.9	188.3	1.9*	377	< 0.1	160
	Microbial 4 y	7.9	83.3	3.9	< 40	0.13	< 1000
	Bentonite 1 y	8.5	332.6	3.5	287		130
	Bentonite 2 y	8.9	196.0	1.8*	375	< 0.1	270
	Bentonite 4 y	8.0	94.9	3.8	< 40	0.06	< 1000
	Abiotic 1 y	8.7	343.5	3.7	222		410
	Abiotic 2 y	9.6	379.5	2.0*	370	< 0.1	170
	Abiotic 4 y	8.2	312.3	4.4	380	< 0.08	< 1000

* Systematically low values, likely not realiable.

However, in the fourth-year microcosms the sulfide concentration in water phase was above the detection limit (> 0.1 mg L^{-1}) in all microcosms except for the anoxic abiotic ones. The highest sulfide concentrations were found in anoxic microbial and bentonite microcosms (0.5 mg L^{-1}). Active, ongoing sulfate reduction was determined using labeled $^{35}SO_4$ in the first-year anoxic microbial duplicate microcosms water phases and sulfate reduction rates of 0.014 and 0.064 nmol mL^{-1} day^{-1} were observed. In one year these rates result in sulfide production of 0.4 to 6.4 μmol per microcosm. No active sulfate reduction was detected in the second-year microcosms. Total iron levels were low in all microcosm waters (<1.0 mg L^{-1}).

DOC concentrations (Fig. 3) in microcosm water phase after two weeks (approximately 50 mg L^{-1}) were notably higher than in the original water mixtures (around 6 mg L^{-1}, Table S2) that were added to the microcosms indicating organic carbon dissolution or microbial carbon metabolism from the bentonite. In the anoxic experiment the DOC concentrations during the first two years were relatively stable and lower than in the oxic microcosms. The first additions of acetate and formate to the microcosms occurred after 32 months. Theoretically the amount of added carbon from the acetate amendment (acetate-C) was 192 mg L^{-1} and from formate amendment (formate-C) 96 mg L^{-1}, which were close to the measured concentrations of acetate-C and formate-C in the oxic abiotic microcosms. In anoxic abiotic microcosms the concentrations of acetate-C and formate-C were lower than in the oxic abiotic microcosms but notably higher than in the microbial or bentonite microcosms. In both anoxic and oxic microbial and bentonite microcosms the detected concentration of carbon from formate was lower (<27% left of added) than the detected concentration of carbon from acetate (44 to 70% left of added) when compared to the added amounts.

3.3. Evolution of microbial communities

3.3.1. Estimated number of bacteria, archaea, fungi and sulfate reducers

The amount of bacterial 16S rRNA genes at the beginning of the experiment varied in the anoxic microcosms from 5.9×10^8 gene copies g^{-1} dw (dry weight) of bentonite to one order of magnitude lower counts in the abiotic control microcosms (Fig. 4). Generally, the gene copy counts were the lowest during the first and the second year, and the addition of electron donors after the second year, increased the bacterial 16S rRNA gene copy counts notably in all anoxic and oxic microcosm types. The change in the size of the sulfate reducing prokaryote (SRP) community estimated from the counts of *dsr*B genes followed the same trend as the bacterial 16S rRNA gene copy counts, although two to three orders of magnitude lower (10^4 to 10^7 gene copies g^{-1} dw of bentonite) (Fig. 4). In the oxic microcosms the *dsr*B genes were detected from the bentonite and microbial microcosms sporadically at the start of the experiment and frequently after the second year. Due to the electron donor additions, the *dsr*B gene counts increased in these microcosms with two to four orders of magnitude by the end of the fourth year. Archaea were detected only in the anoxic microbial microcosms over the whole four-year duration of the experiment with gene copy counts ranging from 1.7×10^4 to 2.9×10^5 g^{-1} dw of bentonite. Likewise, fungal 5.8S rRNA genes were detected from the bentonite microcosms only until the second year and quite sporadically in different microcosm types (Fig. 4). From the original dry bentonite the bacterial, archaeal, fungal and *dsr*B marker gene counts were below method detection level.

3.3.2. Bacterial community

Amplicon sequencing produced relatively low sequence counts especially from the abiotic microcosm types, despite efforts to re-sequence the amplicon libraries of these samples (Table S3). Most bacterial sequences were detected from the anoxic groundwater and oxic surface water mixtures (1907 to 3952 reads) and microbial microcosm at the start (471 to 9754 reads). Bacterial OTU (operational taxonomic unit) numbers detected were the highest in the oxic surface water (329 to 542 OTUs) and the lowest in the oxic abiotic microcosms (0 to 36 OTUs). According to the Chao1 richness estimate, the coverage of the detected bacterial OTUs was mostly less than 40%. The Shannon diversity index for bacteria was low in the anoxic groundwater mixture (1.5 to 2.0) and the highest in the oxic surface water mixture (5.8 to 6.1) and between those in the bentonite microcosms.

Bacterial microbiomes of the anoxic microbial microcosms at the start (Fig. 5) were predominated by the Desulforomonadacea family that had the highest relative abundance together with *Desulfurivibrio* and *Sulfurimonas*. The *Sulfurimonas* genus likely originated from the used anoxic groundwater mixture where it dominated the microbiome whereas its relative abundance decreased in the microbial microcosms over time. Of the three bacterial groups dominating in the anoxic microbial microcosms at the start, only the *Desulfurivibrio* genus was detected at the end of the experiment at quite high relative abundance together with the genera *Trichloromonas*, *Candidatus* Deferrimonas, *Desulfovibrio*, *Desulfomicrobium*, unclassified Desulfarculaceae, *Acetobacterium*, and *Thermincola*. In the anoxic bentonite microcosms where the added groundwater mixture was sterile filtered, spore forming bacteria from the Firmicutes phylum had higher relative abundance than in other microcosm types (Fig. S12). At the beginning of the experiment the relative abundance of *Desulfotomaculum* and unclassified Firmicutes were elevated (Fig. 5). Over time the relative share of

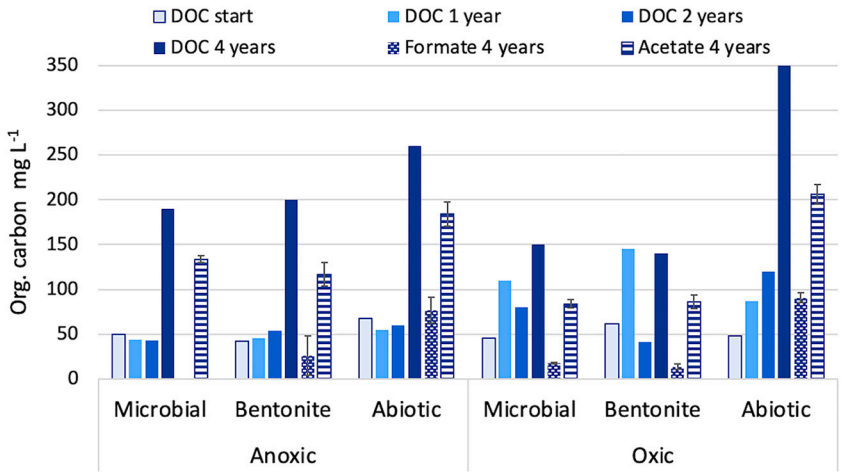

Fig. 3. Dissolved organic carbon (DOC), acetate and formate (as carbon) concentrations in water phase of anoxic and oxic bentonite microcosms as a function of time. DOC measurements were performed for combined (from 3 to 5 microcosms) water samples and acetate and formate measurements for triplicate microcosm water samples.

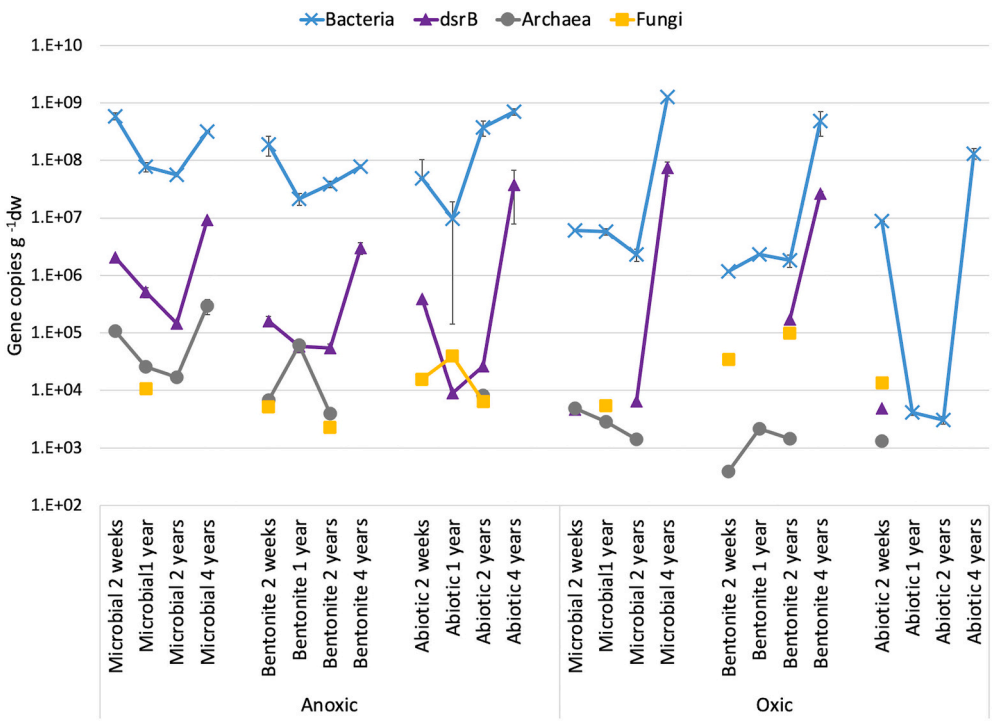

Fig. 4. Estimated bacterial 16S rRNA, *dsr*B, and archaeal 16S rRNA and fungal 5.8S rRNA gene copy counts g^{-1} dw from bentonite slurries of anoxic and oxic bentonite microcosms as a function of time analyzed with quantitative PCR (qPCR). Measurements were performed from triplicate microcosms with triplicate PCR reactions. After 2 years and 8 months of incubation the microcosms were amended with electron donors every fourth month.

Thermicola, *Desulfurispora*, *Desulfosporosinus*, *Pseudomonas* and *Desulfallas-Sporotomaculum* increased. In the abiotic anoxic microcosms *Sulfurimonas* was the most common genus at the start and after the first year. In the second and fourth year its relative abundance was low and instead genera of the Phylum *Nitrospirota* as well as the *Candidatus* Deferrimonas and *Desulfurivibrio* genera showed increased relative abundance in different microcosms.

The bacterial communities in the oxic microcosms were different from those in the anoxic microcosms being dominated by Actinobacteriota and Proteobacteria phyla that had high relative abundance also in the water mixture added to the microcosms (Fig. S11). Only a few genera had high relative abundance and the majority of the detected bacterial groups were present at low relative abundance. The actinobacterial family Sporichthyaceace had the highest relative abundance in the bacterial community of the used oxic water (Fig. 6) and was prominent also in the oxic abiotic microcosms together with the *Limnobacter* genus. These groups were present in the microbial and bentonite microcosms but groups such as *Pseudomonas* and Pseudomonadaceae were dominant at the start, *Sulfurifustis* during and the uncultured Microtrichales and *Pelotomaculum* at the end of the experiment duration.

3.3.3. Archaeal and fungal communities

Amplicon sequencing produced low sequence counts from most archaeal and fungal amplicon libraries, despite efforts to re-sequence the amplicon libraries of these samples (Table S3). Most archaeal sequences and OTUs were identified from the anoxic water mixture (1187 to 2672 reads and 160 to 261 OTUs) and less from the oxic water mixture (164 to 193 reads and 116 to 155 OTUs) and notably less from the anoxic microbial microcosms (116 to 1257 reads and 8 to 32 OTUs). Most fungal sequences were detected in the anoxic water mixture (178 to 884 reads) and only a low number of fungal sequences were found from the oxic water mixture (2 to 5 reads). In bentonite microcosms the fungal sequences were detected irregularly and with low numbers (<255 reads). However, bentonite seemed to increase the sequence read count in the oxic experiment microbial and bentonite microcosms compared to added water mixture. Both fungal and archaeal results were affected by the low sequence read counts and mostly the results only show those groups that likely are the most common in these microbiomes. The archaeal communities of the anoxic water mixture contained groups such as Thermoplasmata, Altiarchaeum, Methanoperedenaceae, Woesearchaeales, but a high number of reads remained as unclassified Archaea (Fig. S13). The most prominent genus was *Methanolobus*, and Bathyarchaeia and Methanoperedenaceae contributed with lower relative abundances in anoxic microbial microcosms throughout the experiment. Oxic microcosms consisted mostly of unclassified Archaea and *Candidatus* Nitrocosmicus until the second year whereafter no archaeal sequences were detected. The fungal community (Fig. S14) of the anoxic water mixture contained a high relative abundance of the Nectriaceae family and low relative abundance of other fungal families. Chaetomiaceae and Malasseziaceae were often detected from the bentonite microcosms, while other families were found only sporadically.

3.3.4. Iron speciation

Iron speciation in bentonite samples was determined on the basis of XANES experiments at the Fe K-edge (Fig. 7) along the pure Fe(II) and Fe (III) references spectra of $CaFe^{(II)}Si_2O_6$ and $Fe^{(III)}{}_2O_3$. All bentonite XANES spectra had similar shape and features, close to a mixture of the two reference spectra. Their white line maximum was however changing as a function of the average iron speciation, being closer to each reference when the corresponding speciation dominate. The spectral features being almost similar for all samples and references, linear combination fittings (LCF) were performed to extract iron speciation from XANES spectra (Table 4). Such approach is however sensitive to the choice of reference samples due to the difference in local environment reflecting on XANES spectral features superimposing the chemical shift expected with change of iron speciation. To assess LCF procedure accuracy, the Fe_3O_4 spectrum was used as a sensitivity test which gave the expected values for Fe_3O_4, validating the procedure. It should be noticed that accuracy of LCF approach remains limited to few % in best case.

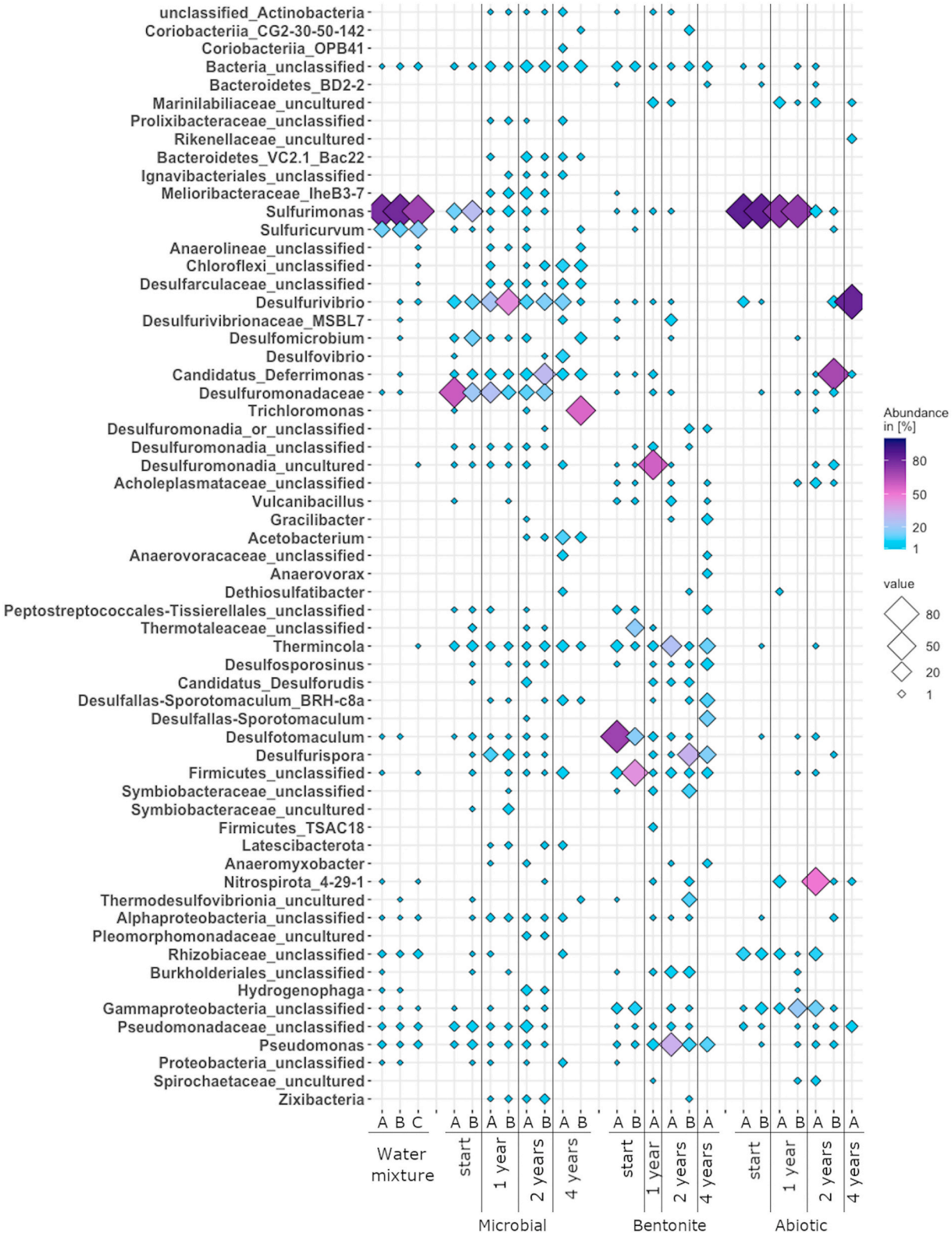

Fig. 5. Relative abundance of bacterial genera in the original anoxic water mixtures and in anoxic microcosms studied over time. The bacterial groups are presented on the left of the graph and the relative abundances of the different genera are represented by a gradient shading and size of the diamonds.

3.3.5. Smectite to illite reaction

Wyoming-type bentonite includes illite (Kiviranta and Kumpulainen, 2011) c. 0.1%. The small amount of illite was not visible in the qualitative mineral identification of the starting material. Purified starting material contained smectite, halite and minor amount of quartz (Fig. S1). Halite (NaCl) was added to the bentonite in purification process and it was found as a remainder in all samples. Based on XRD-diffractograms, clay minerals in all microcosms contained pure smectite and illite with no mixed-layer clay minerals (Moore and Reynolds, 1997). Mg saturation and EG treatment moved the smectite 12.4 Å

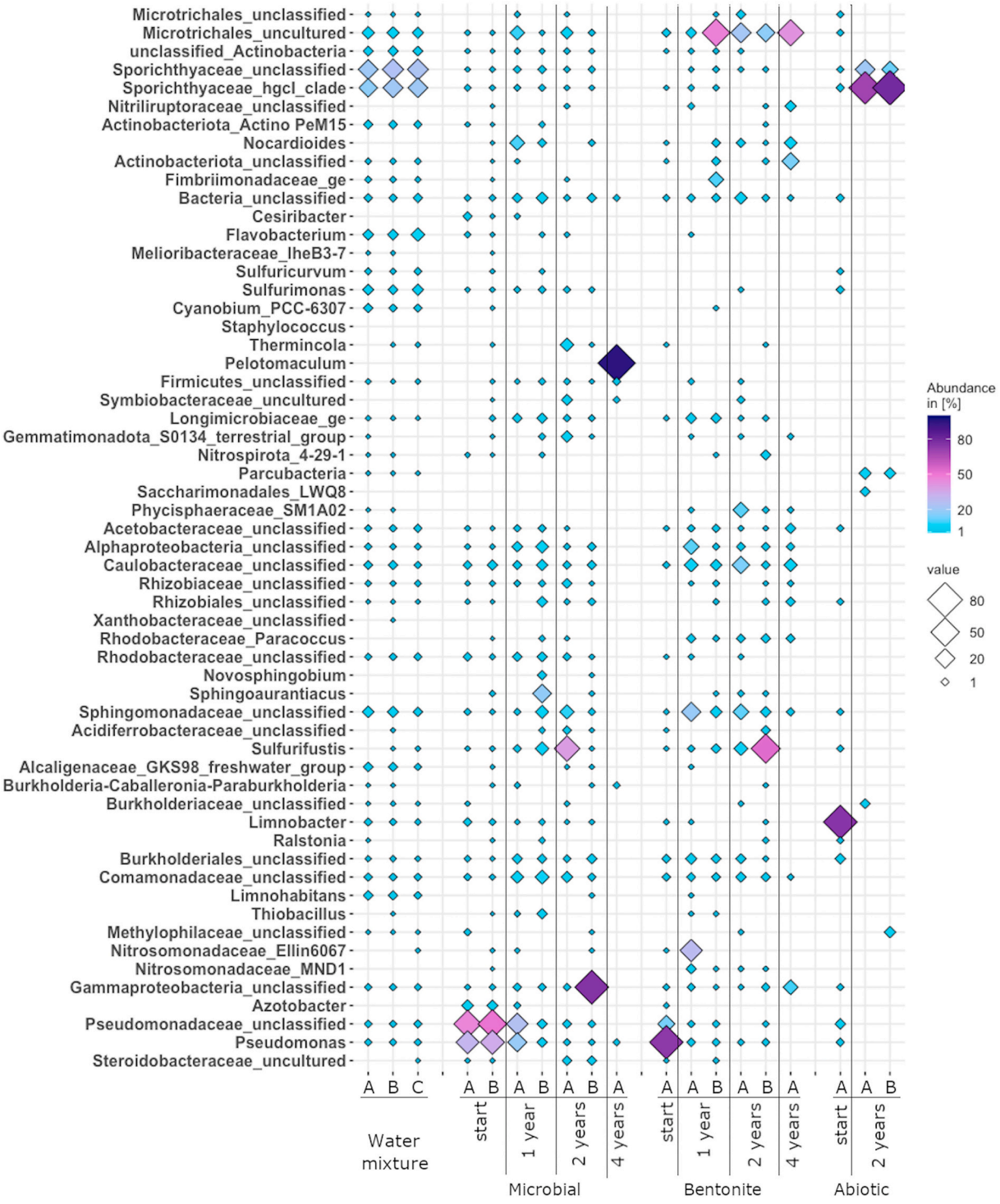

Fig. 6. Relative abundance of bacterial genera in the original oxic water mixtures and in oxic microcosms over time. The bacterial groups are presented on the left of the graph and the relative abundances of the different genera are represented by a gradient shading and size of the diamonds.

reflection to 14.1 Å and further to 16.8 Å. In K saturation the smectite reflection of 11.3 Å collapsed at 200 °C to 10.0 Å and further at 550 °C to 9.7 Å (Fig. S12). 10 Å illite reflection can be seen as a minor reflection in some slurry samples and in all Mg saturated samples as a shoulder in K saturated sample. There was no evidence found of mixed-layer illite-smectite in any of the experiment samples. An indication of illite to smectite ratio being higher especially in the anoxic microbial and bentonite microcosms than in the anoxic abiotic or oxic microcosms or in the starting material was detected with the XRD (Fig. 8).

4. Discussion

The experimental set-up simulating the Finnish nuclear waste geological repository conditions, had microbially active and less active periods, resulting in significant iron reduction of the montmorillonite in bentonite. The fastest measurable change in the anoxic microbial and bentonite microcosms was the disappearance of hydrogen from the gas phase in less than two weeks. Hydrogen as an electron donor is used by many anaerobic microbial groups such as sulfate, sulfur and ferric iron

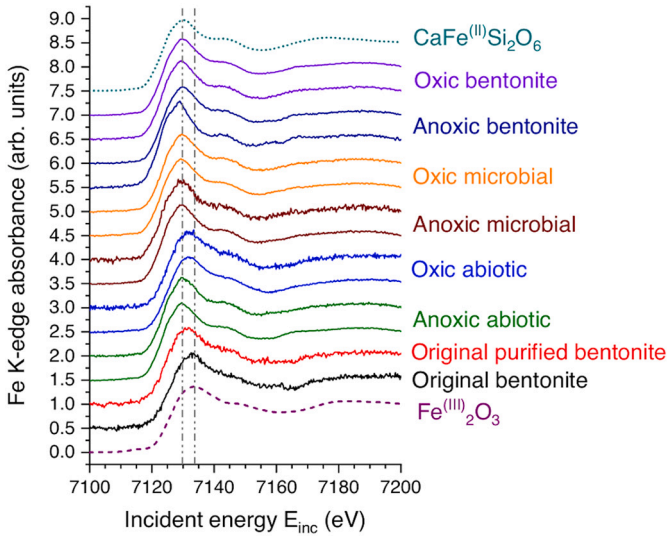

Fig. 7. Fe K-edge XANES spectra of bentonite samples, $CaFe^{(II)}Si_2O_6$ and $Fe^{(III)}{}_2O_3$. Vertical lines refer to the white line maximum as found for $Fe^{(II)}$ and $Fe^{(III)}$ pure valence state references. Spectra are vertically shifted for sake of comparison.

Table 4
Linear combination fitting (LCF) results of purified bentonites from parallel microcosms and of single purified and unpurified original bentonites using $CaFe^{(II)}Si_2O_6$ and $Fe^{(III)}{}_2O_3$ as reference samples. All values are in % of total iron in samples. Fe_3O_4 was here used as a speciation sensitivity test of the LCF procedure, expected values being 33% $Fe^{(II)}$ and 67% $Fe^{(III)}$. Values in parenthesis are uncertainties (%) as deduced from LCF procedure.

	$Fe^{(III)}{}_2O_3$		$CaFe^{(II)}Si_2O_6$	
Sample	A	B	A	B
Anoxic microbial	0 (5)	0 (3)	100 (5)	100 (3)
Anoxic bentonite	0 (5)	0 (2)	100 (5)	100 (2)
Anoxic abiotic	0 (2)	0 (2)	100 (2)	100 (2)
Oxic microbial	0 (2)	0 (3)	100 (2)	100 (3)
Oxic bentonite	0 (2)	0 (2)	100 (2)	100 (2)
Oxic abiotic	52 (3)	53 (3)	48 (3)	47 (3)
Original bentonite	38 (3)		62 (3)	
Original unpurified bentonite	76 (3)		24 (3)	
Fe_3O_4	67(3)		33 (3)	

reducers, methanogens and acetogens (reviewed by Schwartz et al., 2013). This indicated that the microorganisms were active in the anoxic microcosms at the beginning of the experiment and likely SRP were part of this active community as also a thin black layer, likely formed from produced sulfide reacting with ferric iron, was visible on the bentonite surface in microbial microcosms within weeks (Fig. S3).

The deep subsurface crystalline bedrock fracture groundwaters at the Finnish final spent nuclear fuel repository site are oligotrophic (Table S2; Miettinen et al., 2015) and microbial activity level is low. Simulating such microbial communities together with the aim to enhance the microbial activity to create microbial effects in a few years-time, compared to the tens of thousands of years in the final waste disposal repository was a challenge. By adding a low concentration of electron donors, less than a tenth of the DOC measured in the microcosms' water phase at the beginning, activation of inherent oligotrophic microorganisms was targeted. This addition likely benefited Desulfobacterota in the anoxic microcosms. Especially three bacterial groups, Desulfuromonadaceae, *Desulfomicrobium* and *Desulfurivibrio* profited the electron donors added (Fig. 5). These groups include genera that have a role in sulfur and metal cycles (Greene, 2014), are SRP that use H_2, CO_2 or formate and require acetate or yeast extract as an additional carbon source for growth (Galushko and Kuever, 2021) and perform different sulfur species reduction and sulfur disproportionation reactions using acetate or inorganic CO_2 as a carbon source (Melton et al., 2016). Based on the increment of the relative abundances of these bacterial groups the addition of acetate and formate likely enhanced the hypothesized bentonite structure affecting sulfidogenic and iron reducing microorganisms at the beginning of the experiment. Methanol addition seemed to increase the relative abundance of the archaeal *Methanolobus* genus as it is a methylotrophic methanogen (Oren, 2014) and it is likely that the thriving of this genus did not affect the bentonite.

After one-year, active ongoing sulfate reduction was detected with labeled $^{35}SO_4$ in anoxic microbial microcosms' water phase. However, no active sulfate reduction was detected in the second-year microcosms, which indicated that electron donors needed for sulfate reduction were exhausted and the DOC dissolving from the bentonite did not support sulfate reduction, at least in the water phase. This was also supported by the chemical data (Table 2) as the sulfate concentrations and redox values increased in the water phase and the visible image of anoxic microbial and bentonite microcosms was brownish. Moreover, the estimated bacterial 16S rRNA and sulfate reducer (*dsr*B) gene counts were decreasing since the start of the experiment (Fig. 3). Such activity decrease was not expected as the bentonite and the crushed rock were thought to offer nutrients and energy sources. The DOC values measured in the water phase were relatively high (above 40 mg L^{-1} all times) and inorganic carbon, in addition to sulfate, was dissolving from the bentonite (Melamed and Pitkänen, 1996; Vikman et al., 2018), which could be utilized by autotrophic microorganisms. The easily utilizable part of the DOC did not, however, support the microbial activity anymore during the second year in the anoxic microcosms. Maanoja et al. (2020) also concluded that DOC from Wyoming-type bentonite enhanced microbial growth as in uninoculated bentonite cells the DOC values were higher than in inoculated bentonite cells. Organic carbon dissolved more efficiently in the oxic microcosms than in anoxic microcosms as the DOC levels remained around 50 mg L^{-1} in the anoxic abiotic microcosms whereas increased over time from 50 to over 100 mg L^{-1} in oxic abiotic microcosms in two years, possibly due to lower ionic strength in oxic microcosms (Cincotta et al., 2019). However, it is challenging to assess the level of microbial activity in abiotic microcosms and their effect on DOC dissolution and utilization.

The SRR measured after one year ranged from 0.01 to 0.06 nmol mL^{-1} day^{-1} in the anoxic microbial microcosms's water phase which results to a constant rate from 0.4 to 6.4 μmol of sulfide in a year per microcosm. This is a conservative estimate as it is likely that the SRR was already lower at the one-year time point than at the beginning of the experiment due to the ongoing electron donor usage. The Wyoming-type bentonite in the microcosms contained small amounts of ferric iron in biotite, siderite, illite and hornblende. Moreover, the crushed rock added in microcosms entailed biotite, chlorite, garnet and altered Fe-oxides (Fe containing minerals together around 11.2 vol-%) that made it hard to assess the actual amount of ferric iron in the microcosms and its bioavailability or abiotic availability. The estimated ferric iron from all sources in each microcosms was around 2 mmol, which theoretically equals to scavenging of all formed sulfide over a period of 1080 years in the microcosms with the measured SRR of 0.06 nmol mL^{-1} d^{-1}. This SRR is much lower than in natural coastal (2–20 m depths) sediments where electron donors are available, the SRR generally has been found below the order of 20 nmol mL^{-1} d^{-1} (Jørgensen, 1982) whereas from natural deep subsurface oligotrophic environments such information is scarce. In Sevenyui, Eastern Siberia, Russia, deep repository site for liquid radioactive waste (180 to 465 m below sea level), SRR varying between 0.0004 and 0.4 nmol mL^{-1} d^{-1} in different groundwater samples were measured (Nazina et al., 2004), which are plausible rates compared to rate in the bentonite microcosms depending on the electron donor availability. The measured SRR and calculation of the time needed for total iron reduction in the microcosms resulted in an incorrect estimation as all structural iron was reduced in bentonite in less than five years. This is likely due to three reasons, firstly iron was

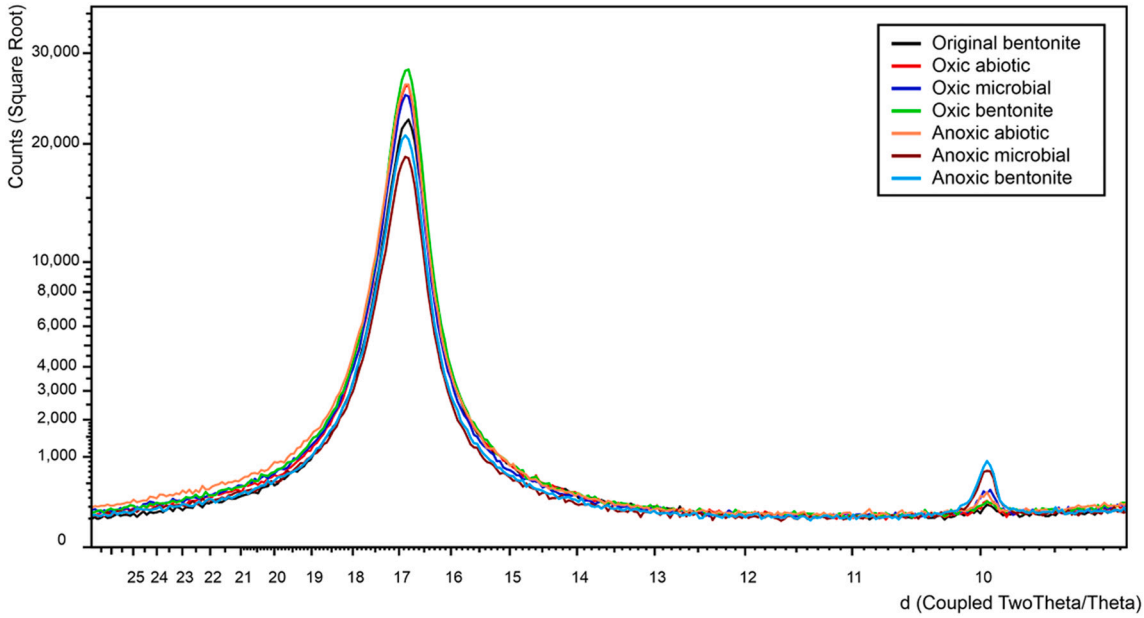

Fig. 8. All Mg saturated and ethylene glycol solvated (60 °C > 16 h) samples had smectite reflection in 16.8 Å and illite reflection at 10 Å. Anoxic microbial and anoxic bentonite samples had the strongest illite reflection compared to other samples.

reduced also by iron reducers, secondly the SRR was higher than the measured rate as it was defined before the electron donor additions started, and thirdly iron speciation was measured on the purified fraction of bentonite excluding crushed rock and bentonite accessory minerals that were included in the theoretical calculation. The iron speciation in the accessory minerals and crushed rock is not known.

The start of supplementing electron donors, acetate and formate (2 mM each at one time), to the bentonite microcosms once every fourth month reactivated the microbial communities in both the anoxic and oxic bentonite experiments. The number of bacterial 16S rRNA and SRP (*dsr*B) gene counts rose clearly, especially in the oxic microcosms where their earlier amounts were lower. Sulfate reduction was likely initiated very rapidly after the electron donor additions as the black coloring, regarded as iron sulfide formation due to sulfate reduction, was detected in anoxic microbial and bentonite microcosms within two weeks (Figs. S3-S4). In the oxic microcosms where no sulfate reduction was detected during the first two years of the experiment, the sulfate reduction was visually detected two months after the start of the electron donor additions (Fig. S6-S7). No black coloring was noted in any of the abiotic microcosms in four years (Fig. S8-S9). Sulfate reduction was maintained during the fourth year based on visual observations, but also redox values were the lowest at the fourth year in all microcosm types (Table 2). In a bentonite slurry microcosm experiment by Matschiavelli et al. (2019) high concentration (50 mM) of added organic carbon compounds inhibited the metabolic activity of inherent microorganisms in the Bavarian bentonite. Only the microcosms supplemented with hydrogen or 10 mM lactate showed sulfate reducing activity that was related to *Desulfosporosinus* and to lesser extent to *Desulfotomaculum* genera. This supports the selection of low concentration of electron donors added in the present study as the predominant and likely active genera were SRP, originating mainly from the groundwater in the anoxic microbial microcosms. By contrast, in the bentonite microcosms where the added groundwater was sterile filtered and microorganisms originated from the bentonite, the main genera detected were spore forming bacteria: *Desulfotomaculum*, *Thermincola, Desulfurispora,* unclassified Firmicutes*, Desulfosporosinus* and Desulfallas-Sporotomaculum group that include many SRP, but also fermenters and genera able to reduce ferric iron (Aüllo et al., 2013; Zavarzina et al., 2007; Wrighton et al., 2008; Spring and Rosenzweig, 2006; Watanabe et al., 2018; Qiu et al., 2003).

The levels of microbially reduced iron in nontronite and ferruginous smectite incubated with iron reducing cultures have been found to be at most 30 to 40% (Huang et al., 2018; Kostka et al., 1996) and up to 71% in Fe-poor Ca-montmorillonite incubated with four iron reducing strains in culture medium (Cui et al., 2018) but mostly the maximum level of reduced iron has been 25–30% (Pentráková et al., 2013). One major difference in these studies has been the limited time frame of the experiments, mostly within few weeks compared to almost five years in the present experiment. The fact, that all structural iron was reduced in the purified and fine part of the montmorillonite in all microbial and bentonite microcosms within five years may have devastating effects on bentonite swelling pressure (Gates et al., 1993; Cui et al., 2018) and thus on its ability to protect the nuclear waste canisters in local low bentonite density areas in the final disposal repository. Nevertheless, the effect of iron reduction on the formation of illite was not considerable but clear, particularly in anoxic samples (Fig. 8). The effects of biological iron reduction have mostly been studied in case of Fe-rich smectites (Kim et al., 2004; Ribeiro et al., 2009; Liu et al., 2012; Huang et al., 2018) and it remains to be studied, how the iron reduction in low iron content smectites affects their performance and especially the swelling ability. The iron speciation results between parallel microcosms were consistent in all cases (Table 4). Small differences between the parallel microcosms are however visible when comparing XANES spectra but are not reflected in the overall speciation quantification via LCF method. This is clearly visible for anoxic bentonite spectra (Fig. 7) for which one may expect differences in the Fe local environment. Whether those differences are related to the real difference between individual microcosms as they were also visually different (Figs. S5-S10) or the bentonite heterogeneity, or both remained unsolved. Conflicting results from the iron speciation measurements of the original bentonites that were studied as such or after anoxic purification may be affected by the bentonite material heterogeneity but also imply that the anoxic purification process affected the iron speciation, which should be further studied.

It has been shown that the reduction of structural iron increases net negative charge in the mineral structure, the hydration of smectite surfaces, and the cation exchange capacity (Gates et al., 1993; Kostka et al., 1999; Stucki et al., 2002). Relatively small CEC increase was detected in the anoxic microbial microcosms already during early stages of the experiment, but the values did not increase during the four-year incubation. However, the change in CEC is not necessarily linear with

the structural Fe(II) content due to the ancillary reactions (Stucki and Kostka, 2006). Such reactions were possible as the redox values were the highest in the second year in anoxic microbial microcosms as well as the coloring of the microcosms turned from grey to brownish and then back to grey/black after electron donor additions.

Anoxic microbial microcosms after four years consisted of known sulfidogenic bacteria (*Desulfurivibrio, Desulfovibrio, Desulfomicrobium, Trichloromonas*, basonym *Desulfuromonas,* unclassified Desulfarculaceae) and genera including known iron reducers *Candidatus* Deferrimonas (Badalamenti et al., 2016) and *Thermincola* (Zavarzina et al., 2007). In anoxic bentonite microcosm the predominating microbiome included spore-forming IRB *Thermicola* and SRP *Desulfurispora*, *Desulfoporosinus* and Desulfallas-Sporotomaculum. The microbial community in the oxic microcosms differed from the anoxic community over the whole duration of the experiment likely due to the initial microbial community composition in water mixtures and oxygen presence at the beginning but also the lower ionic strength affected in the oxic microcosms. The dominant community in the oxic experiment showed scarce SRP or spore-forming bacteria when studied with the amplicon sequencing method. The lack of SRP at the beginning of the experiment was logic as oxygen is toxic for SRP (Marschall et al., 1993) but after oxygen was mostly consumed it was expected that spore-forming SRP had germinated and activated in the microcosms. This was seen during the last year of the experiment as the number of *dsr*B genes increased significantly ($p < 0.02$) and black coloring on the bentonite in the microcosms occurred after electron donor additions (Fig. S5-S6) and the structural iron was reduced also in these microcosms. However, this was not seen by the amplicon sequencing as the SRP and spore-forming bacteria (Firmicutes) were mainly missing (Fig. 6; Fig. S11). Only in one oxic microbial microcosm, a *Pelotomaculum* genus was detected with high relative abundance by amplicon sequencing. *Pelotomaculum* are spore-forming and generally regarded as fermenters and undergoing syntrophy with anaerobic respiring microorganisms or methanogens (Imachi et al., 2007; de Bok et al., 2005). However, an anaerobic, sulfate reducing *Pelotomaculum,* degrading benzene has been discovered (Dong et al., 2017) indicating *Pelotomaculum* as a possible SRP also in bentonite. In addition, aerobic *Sufurifustis* (Umezawa et al., 2016) and Microtrichales related to the microaerophilic *Microthrix* genus (McIlroy et al., 2013; Fan et al., 2020) illustrate the oxic and anoxic changes that occurred in the oxic microcosms over time but also the formation of microenvironments in individual microcosms. Generally, the dominance of different microbial groups in different microcosm types originating from subsurface groundwater, oxic surface water or bentonite show that diverse microbial communities are able to cause the structural iron reduction in bentonite.

The abiotic control microcosms were not assumed sterile as it is known that sterile filtration removes only cells bigger than 0.22 μm and in the deep subsurface, cells smaller than that are frequently detected (Wu et al., 2016; Lopez-Fernandez et al., 2018). In some anoxic abiotic control bottles, 4 years and 10 months after the start, some black coloring was noticed indicating SRP activity (Fig. S10). Already in the fourth-year samples the amount of *dsr*B gene copies was increased in the anoxic abiotic microcosms. It is possible that some of the nano-sized cells (< 0.1 μm) could show SRP activity, but that has not been proposed to our knowledge. SRP activity was evaluated to originate from the heat-treated bentonites (180 °C, 16 h) as the endospores generally are larger (Carrera et al., 2006) than the pore size used for the groundwater filtration. The heat tolerance of spore-forming SRP, indigenous for Wyoming-type bentonite, was verified in dry bentonite in an experiment where bentonite was heated at 100 °C for 20 h and then incubated in rich sulfate reducer medium (27 days, at 20 or 37 °C) whereafter black coloring was observed in bentonite samples indicating sulfate reduction (Masurat et al., 2010). However, similar treatment at 120 °C did not show sulfide formation in bentonites anymore. The notably higher temperature (180 °C) in this study likely caused severe damage to the endospores as the spores took significantly longer to germinate and activate and thus a longer time was needed before the black coloring in the bentonite microcosms was detected, but it nevertheless demonstrated the survival of the endospores after extreme conditions. Furthermore, the reduction of all ferric iron in purified bentonite of abiotic microcosms indicate that the microbial activity after the germination had been fast and likely started earlier than the color change was visible.

In the oxic microbial type microcosms oxygen was consumed from the gas phase faster than in oxic abiotic microcosms but not markedly (Fig. 2B). In addition to microorganisms, also chemical reactions and adsorption are known to affect the gas phase oxygen level in repository conditions (Giroud et al., 2018; Carlsson and Muurinen, 2008; Grandia et al., 2006) and based on the relatively fast oxygen level decrease in the abiotic microcosms these abiotic reactions had notable influence on the removal of oxygen. Ferrous iron bearing minerals, except for biotite, were regarded as the main sink for oxygen together with organic matter and microbial oxygen respiration from the backfill gas phase within a month in numeric simulations (Grandia et al., 2006). In addition, oxidation of dissolved pyrite from Opalinius Clay has been found to be a process controlling oxygen in the gas phase (Giroud et al., 2018). This kind abiotic engagement of oxygen in the bentonite matrix may later offer an electron donor source for microorganisms in repository conditions.

The low sequence counts obtained from the bentonite samples was incoherent with the qPCR results and activation of SRP. DNA extraction from bentonite samples is demanding and protocols are under constant development (Povedano-Priego et al., 2021; Matschiavelli et al., 2019; Engel et al., 2019) and evidently only a part of the community present in the bentonite microcosms was detected. Several commercial DNA extraction kits and other modified DNA extraction protocols (Miettinen et al., 2018) were tested. The selected procedure gave the highest DNA amounts from inoculated bentonite samples but based on the results, further improvement of DNA-extraction is needed. The role of fungi and archaea in the bentonite microcosms seemed not considerable, however the more efficient DNA-extraction method could have influenced the results. Anaerobic heterotrophic fungi are degraders of calcitrant organic compounds such as bentonite and they produce hydrogen gas in their metabolism potentially providing substrates for prokaryotes (Drake and Ivarsson, 2018). Active fungi have been detected from the Olkiluoto subsurface (Sohlberg et al., 2015) and they could in long-term have importance in bentonite environment. *Methanolobus*, a methanogenic archaeon, growing solely on C1-compounds such as methanol (Oren, 2014), unclassified *Methanoperedens* that perform anaerobic methane oxidation (Haroon et al., 2013) and Bathyarchaeia, a generalist that include species able to utilize among others methane and reduce sulfur (Zhou et al., 2018) were detected over the whole duration of the experiment and their role in the community needs further investigation.

5. Conclusions

The aim of this study was to find out if microorganisms inherent for bentonite or repository site anoxic groundwater are able to affect the bentonite structural iron in conditions that simulate nuclear waste geological repository in anoxic and oxic conditions but enable microbial activity with low bentonite density. The change in the structure of the indigenous microbial communities and their effects on the bentonite structural iron were studied over time. The dissolving organic carbon from the bentonite was able to maintain the microbial activity only for less than two years. Regular addition of short-chained organic compounds as electron donors (Na-acetate and formate, 2 mM each, every four months) reactivated the microbial communities and sulfate reduction was visible within two weeks in anoxic microcosms as black color likely due to iron sulfide formed in the bentonite layer. At the end of the experiments (4 years and 10 months) the purified part of the bentonite showed total iron reduction in all microbial microcosms and minor smectite illitization in anoxic microbial microcosms. Microbial

communities causing iron reduction were assumed to be mainly sulfate reducers and likely iron reducers based on their high relative abundance in the anoxic microcosms. However, the community causing the iron reduction in the initially oxic microcosms was not clear. This community was different from the one in the initially anoxic microcosms indicating that the source of the microorganisms causing the iron reduction was not very specific but could originate from different environments. Fungi and archaea seemed not to have a notable role in the community of the studied bentonite microcosms based on their low gene counts.

Data availability

The sequence data has been submitted to the European Nucleotide Archive (http://www.ebi.ac.uk/ena) under study accession number PRJEB48658.

Funding

This research was funded by the Horizon 2020 project MIND through funding from the Euratom research and training programme 2014–2018 under Grant Agreement no. 661880. The research was also funded by the Finnish Research Programme on Nuclear Waste Management 2018 (Geobiocycle) and 2022 (MiBe). The funding bodies did not participate in design, collection, analyses or interpretation of the data, writing the results or decision to submit this article for publication.

Author contributions

Conceptualisation, H.M. and M.V.; Data curation, H.M., M.B. and R.B.; Formal Analysis, H.M., M.T., and R.B.; Funding acquisition, M.V., H.M. and M.B.; Investigation, H.M., M.T., and R.B.; Methodology, H.M., M.B., R.B. and M.T; Project Administration, M.V. and H.M.; Resources, H.M., M.B. and R.B.; Software, M.B. and H.M.; Supervision, M.V.; Validation, H.M.; Visualization, H.M., R.B. and M.T.; Writing—Original Draft, H.M. and R.B.; Writing—Review & Editing, H.M., M.B., M.T. and M.V.

Declaration of Competing Interest

The authors declare that they have no known competing financial interests or personal relationships that could have appeared to influence the work reported in this paper.

Acknowledgements

Mirva Pyrhönen, Kirsti Helosuo and Anna Manninen are warmly thanked for assistance in the laboratory. Atte Mikkelsson is acknowledged for the gas phase analyses. Merja Itävaara and Markus Olin are warmly thanked for launching this research area at VTT. Posiva Ltd. is acknowledged for providing the groundwater samples and Teollisuuden Voima Oyj the surface water from Olkiluoto. Authors thank the Center for x-ray Spectroscopy for providing experiment time and support with the HelXAS spectrometer under Proposal Numbers 2021-0009 and 2021-0005.

Appendix A. Supplementary data

Supplementary data to this article can be found online at https://doi.org/10.1016/j.clay.2022.106465.

References

Amman, L., Bergaya, F., Lagaly, G., 2005. Determination of the cation exchange capacity of clays with copper complexes revisited. Clay Miner. 40, 441–453. https://doi.org/10.1180/0009855054040182.

Aüllo, T., Ranchou-Peyruse, A., Ollivier, B., Magot, M., 2013. *Desulfotomaculum* spp. and related gram-positive sulfate-reducing bacteria in deep subsurface environments. Front. Microbiol. 4, 362. https://doi.org/10.3389/fmicb.2013.00362.

Badalamenti, J.P., Summers, Z.M., Chan, C.H., Gralnick, J.A., Bond, D.R., 2016. Isolation and genomic characterization of '*Desulfuromonas soudanensis* WTL', a metal- and electrode-respiring bacterium from anoxic deep subsurface brine. Front. Microbiol. 7, 913. https://doi.org/10.3389/fmicb.2016.00913.

Bengtsson, A., Pedersen, K., 2017. Microbial sulphide-producing activity in water saturated Wyoming MX-80, Asha and Calcigel bentonites at wet densities from 1500 to 2000 kg m^{-3}. Appl. Clay Sci. 137, 203–212. https://doi.org/10.1016/j.clay.2016.12.024.

Bomberg, M., Miettinen, H., 2020. Data on the optimization of an archaea-specific probe-based qPCR assay. Data in Brief. 33, 106610 https://doi.org/10.1016/j.resmic.2020.07.001.

Bomberg, M., Lamminmäki, T., Itävaara, M., 2015. Estimation of microbial metabolism and co-occurrence patterns in fracture groundwaters of deep crystalline bedrock at Olkiluoto, Finland. Biogeosci. Discuss. 12, 13819–13857. https://doi.org/10.5194/bgd-12-13819-2015.

Bomberg, M., Lamminmäki, T., Itävaara, M., 2016. Microbial communities and their predicted metabolic characteristics in deep fracture groundwaters of the crystalline bedrock at Olkiluoto, Finland. Biogeosciences 13, 6031–6047. https://doi.org/10.5194/bg-13-6031-2016.

Carlsson, T., Muurinen, A., 2008. Identification of Oxygen-Depleting Components in MX-80 Bentonite, 1124, 502. https://doi.org/10.1557/PROC-1124-Q05-02. MRS Online Proceedings Library.

Carpén, L., Rajala, P., Bomberg, M., 2018. Corrosion of copper in anoxic ground water in the presence of SRB. Corros. Sci. Technol. 17, 147–153. https://doi.org/10.14773/cst.2018.17.4.147.

Carrera, M., Zandomeni, R.O., Fitzgibbon, J., Sagripanti, J.-L., 2006. Difference between the spore sizes of *Bacillus anthracis* and other Bacillus species. J. Appl. Microbiol. 102, 303–312. https://doi.org/10.1111/j.1365-2672.2006.03111.x.

Cincotta, M.M., Perdrial, J.N., Shavitz, A., Libenson, A., Landsman-Gerjoi, M., Perdrial, N., Armfield, J., Adler, T., Shanley, J.B., 2019. Soil aggregates as a source of dissolved organic carbon to streams: an experimental study on the effect of solution chemistry on water extractable carbon. Front. Environ. Sci. 7, 172. https://doi.org/10.3389/fenvs.2019.00172.

Cui, K., Sun, S., Xiao, M., Liu, T., Xu, Q., Dong, H., Wang, D., Gong, Y., Sha, T., Hou, J., Zhang, Z., Fu, P., 2018. Microbial mineralization of montmorillonite in low-permeability oil reservoirs for microbial enhanced oil recovery. Appl. Environ. Microbiol. 84 https://doi.org/10.1128/AEM.00176-18 e00176-18.8.

de Bok, F.A.M., Hemie, J.M., Harmsen, J.M., Plugge, C.M., de Vries, M.C., Akkermans, A.D.L., de Vos, W.M., Stams, A.J.M., 2005. The first true obligately syntrophic propionate-oxidizing bacterium, *Pelotomaculum schinkii* sp. nov., co-cultured with *Methanospirillum hungatei*, and emended description of the genus *Pelotomaculum*. Int. J. Syst. Evol. Microbiol. 55, 1697–1703. https://doi.org/10.1099/ijs.0.02880-0.

Dong, H., 2012. Clay-microbe interactions and implications for environmental mitigation. Elements 8, 113–118. https://doi.org/10.2113/gselements.8.2.113.

Dong, X., Dröge, J., Con Toerne, C., Marozava, S., McHardy, A.C., Meckenstock, R.U., 2017. Reconstructing metabolic pathways of a member of the genus *Pelotomaculum* suggesting its potential to oxidize benzene to carbon dioxide with direct reduction of sulfate. FEMS Microbiol. Ecol. 93 (3) https://doi.org/10.1093/femsec/fiw254, 2017 Mar 1.

Drake, H., Ivarsson, M., 2018. The role of anaerobic fungi in fundamental biogeochemical cycles in the deep biosphere. Fungal Biol. Rev. 32, 20–25. https://doi.org/10.1016/j.fbr.2017.10.001, 17.

Engel, K., Coyotzi, S., Vachon, M.A., McKelvie, J.R., Neufeld, J.D., 2019. Validating DNA extraction protocols for bentonite clay. mSphere 4. https://doi.org/10.1128/mSphere.00334-19 e00334-19.

Fan, N.-S., Qi, R., Huang, B.-C., Jin, R.-C., Yang, M., 2020. Factors influencing *Candidatus Microthrix parvicella* growth and specific filamentous bulking control: a review. Chemosphere. 244, 125371 https://doi.org/10.1016/j.chemosphere.2019.125371.

Galushko, A., Kuever, J., 2021. Desulfomicrobium. In: Trujillo, M.E., Dedysh, S., DeVos, P., Hedlund, B., Kämpfer, P., Rainey, F.A., Whitman, W.B. (Eds.), Bergey's Manual of Systematics of Archaea and Bacteria. https://doi.org/10.1002/9781118960608.gbm01032.pub2.

Gates, W.P., Wilkinson, H.T., Stucki, J.W., 1993. Swelling properties of microbially reduced ferruginous smectite. Clay Clay Miner. 41, 360–364. https://doi.org/10.1346/CCMN.1993.0410312.

Geets, J., Borremans, B., Diels, L., Springael, D., Vangronsveld, J., Van Der Lelie, D., Vanbroekhoven, K., 2006. DsrB gene-based DGGE for community and diversity surveys of sulfate-reducing bacteria. J. Microbiol. Methods 66, 194–205. https://doi.org/10.1016/j.mimet.2005.11.002.

Giroud, N., Tomonaga, Y., Wersin, P., Briggs, S., King, F., Vogt, T., Diomidis, N., 2018. On the fate of oxygen in a spent fuel emplacement drift in Opalinus Clay. Appl. Geochem. 97, 270–278. https://doi.org/10.1016/j.apgeochem.2018.08.011.

Grandia, F., Domènech, D., Arcos, D., Duro, L., 2006. Assessment of the oxygen consumption in the backfill. Geochemical modelling in a saturated backfill. SKB Report R-06-106. https://www.skb.com/publication/1287051/R-06-106.pdf (accessed on September 7th, 2021).

Greene, A.C., 2014. The Family *Desulfuromonadaceae*. In: Rosenberg, E., DeLong, E.F., Lory, S., Stackebrandt, E., Thompson, F. (Eds.), The Prokaryotes. Springer, Berlin, Heidelberg. https://doi.org/10.1007/978-3-642-39044-9_380.

Grigoryan, A.A., Jalique, D.R., Medihala, P., Stroes-Gascoyne, S., Wolfaardt, G.M., McKelvie, J., Korber, D.R., 2018. Bacterial diversity and production of sulfide in microcosms containing uncompacted bentonites. Heliyon 4, e00722. https://doi.org/10.1016/j.heliyon.2018.e00722.

Haroon, M.F., Hu, S., Shi, Y., Imelfort, M., Keller, J., Hugenholtz, P., Yuan, Z., Tyson, G. W., 2013. Anaerobic oxidation of methane coupled to nitrate reduction in a novel archaeal lineage. Nature 500, 567–572. https://doi.org/10.1038/nature12375.

Huang, L., Feng, C., Jiang, H., Dong, H., Liu, Z., Zeng, Q., 2018. Reduction of structural Fe(III) in nontronite by thermophilic microbial consortia enriched from hot springs in Tengchong, Yunnan Province, China. Chem. Geol. 479, 47–57. https://doi.org/10.1016/j.chemgeo.2017.12.028.

Imachi, H., Sakai, S., Ohashi, A., Harada, H., Hanada, S., Kamagata, Y., Sekiguchi, Y., 2007. *Pelotomaculum propionicicum* sp. nov., an anaerobic, mesophilic, obligately syntrophic, propionate-oxidizing bacterium. Int. J. Syst. Evol. Microbiol. 57, 1487–1492. https://doi.org/10.1099/ijs.0.64925-0.

Jørgensen, B.B., 1982. Mineralization of organic-matter in the sea bed – the role of sulfate reduction. Nature 296, 643–645. https://doi.org/10.1038/296643a0.

Kim, J., Dong, H., Seabaugh, J., Newell, S.W., Eberl, D.D., 2004. Role of microbes in the smectite-to-illite reaction. Science 303, 830–832. https://doi.org/10.1126/science.1093245.

Kiviranta, L., Kumpulainen, S., 2011. Quality control and characterization of bentonite materials. Posiva Working Report 2011-84. Downloadable from. https://www.posiva.fi/en/index/media/reports.html (accessed on September 7th, 2021).

Kõljalg, U., Nilsson, R.H., Abarenkov, K., Tedersoo, L., Taylor, A.F.S., Bahram, M., Bates, S.T., Bruns, T.D., Bengtsson-Palme, J., Callaghan, T.M., Douglas, B., Drenkhan, T., Eberhardt, U., Dueñas, M., Grebenc, T., Griffith, G.W., Hartmann, M., Kirk, P.M., Kohout, P., Larsson, E., Lindahl, B.D., Lücking, R., Martín, M.P., Matheny, P.B., Nguyen, N.H., Niskanen, T., Oja, J., Peay, K.G., Peintner, U., Peterson, M., Põldmaa, K., Saag, L., Saar, I., Schüßler, A., Scott, J.A., Senés, C., Smith, M.E., Suija, A., Taylor, D.L., Telleria, M.T., Weiss, M., Larsson, K.H., 2013. Towards a unified paradigm for sequence-based identification of fungi. Mol. Ecol. 22, 5271–5277. https://doi.org/10.1111/mec.12481.

Kostka, J.E., Stucki, J.W., Nealson, K.H., Wu, J., 1996. Reduction of structural Fe(III) in smectite by a pure culture of *Shewanella putrefaciens* strains MR-1. Clay Clay Miner. 44, 522–529. https://doi.org/10.1346/CCMN.1996.0440411.

Kostka, J.E., Wu, J., Nealson, K.H., Stucki, J.W., 1999. The impact of structural Fe(III) reduction by bacteria on the surface chemistry of smectite clay minerals. Geochim. Cosmochim. Acta 63, 3705–3713. https://doi.org/10.1016/S0016-7037(99)00199-4.

Lever, M.A., Torti, A., Eickenbusch, P., Michaud, A.B., Šantl-Temkiv, T., Jørgensen, B.B., 2015. A modular method for the extraction of DNA and RNA, and the separation of DNA pools from diverse environmental sample types. Front. Microbiol. 6, 476 https://doi.org/10.3389/fmicb.2015.00476.

Liu, D., Dong, H., Bishop, M.E., Zhang, J., Wang, H., Xie, S., Wang, S., Huang, L., Eberl, D.D., 2012. Microbial reduction of structural iron in interstratified illite-smectite minerals by a sulfate-reducing bacterium. Geobiology 10, 150–162. https://doi.org/10.1111/j.1472-4669.2011.00307.x.

Lloyd, J.R., Cherkouk, A., 2020. Introduction. In: Lloyd, J.R., Cherkouk. (Eds.), The Microbiology of Nuclear Waste Disposal. Elsevier, Amsterdam, Oxford, Cambridge.

Lopez-Fernandez, M., Broman, E., Turner, S., Wu, X., Bertilsson, S., Dopson, M., 2018. Investigation of viable taxa in the deep terrestrial biosphere suggests high rates of nutrient recycling. FEMS Microbiol. Ecol. 94, fiy121. https://doi.org/10.1093/femsec/fiy121.

Maanoja, S., Lakaniemi, A.-M., Lehtinen, L., Salminen, L., Auvinen, H., Kokko, M., Palmroth, M., Muuri, E., Rintala, J., 2020. Compacted bentonie as a source of substrates for sulfate-reducing microorganisms in a simulated excavation-damaged zone of a spent nuclear fuel repository. Appl. Clay Sci. 196, 105746. https://doi.org/10.1016/j.clay.2020.105746.

Marschall, C., Frenzel, P., Cypionka, H., 1993. Influence of oxygen on sulfate reduction and growth of sulfate-reducing bacteria. Arch. Microbiol. 159, 168–173. https://doi.org/10.1007/BF00250278.

Masurat, P., Eriksson, S., Pedersen, K., 2010. Evidence of indigenous sulphate-reducing bacteria in commercial Wyoming bentonite MX-80. Appl. Clay Sci. 47, 51–57. https://doi.org/10.1016/j.clay.2008.07.00.

Matschiavelli, N., Kluge, S., Podlech, C., Standhaft, D., Grathoff, G., Ikeda-Ohno, A., Warr, L.N., Chukharkina, A., Arnold, T., Cherkouk, A., 2019. The year-long development of microorganisms in uncompacted Bavarian bentonite slurries at 30 and 60°C. Environ. Sci. Technol. 53, 10514–10524. https://doi.org/10.1021/acs.est.9b02670.

McIlroy, S.J., Kristiansen, R., Albertsen, M., Karst, S.M., Rossetti, S., Lund Nielsen, J., Tandoi, V., Seviour, R.J., p.H. Nielsen., 2013. Metabolic model for the filamentous '*Candidatus* Microthrix parvicella' based on genomic and metagenomic analyses. ISME J 7, 1161–1172. https://doi.org/10.1038/ismej.2013.6.

Meier, L.P., Kahr, G., 1999. Determination of the cation exchange capacity (CEC) of clay minerals using the complexes of copper(II) ion with triethylenetetramine and tetraethylenepentamine. Clay Clay Miner. 47, 386–388. https://doi.org/10.1346/CCMN.1999.0470315.

Melamed, A., Pitkänen, P., 1996. Chemical and mineralogical aspects of water-bentonite interaction in nuclear fuel disposal conditions. VTT Technical Research Centre of Finland. Research Notes no. 1766. http://www.vtt.fi/inf/pdf/tiedotteet/1996/T1766.pdf (accessed on September 7th, 2021).

Melton, E.D., Sorokin, D.Y., Overmars, L., Chertkov, O., Clum, A., Pillay, M., Ivanova, N., Shapiro, N., Kyrpides, N.C., Woyke, T., Lapidus, A.L., Muyzer, G., 2016. Complete genome sequence of *Desulfurivibrio alkaliphilus* strain AHT2(T), a haloalkaliphilic sulfidogen from Egyptian hypersaline alkaline lakes. Stand. Genomic Sci. 11, 67. https://doi.org/10.1186/s40793-016-0184-4.

Miettinen, H., Bomberg, M., Nyyssönen, M., Salavirta, H., Sohlberg, E., Vikman, M., Itävaara, M., 2015. The diversity of microbial communities in Olkiluoto bedrock groundwaters 2009–2013. Working report 2015-12. Posiva Ltd: Eurajoki, Finland, 2015; p. 160. Downloadable from. https://www.posiva.fi/en/index/media/reports.html (accessed on September 7th, 2021).

Miettinen, H., Bomberg, M., Merroun, M., Provedano-Priego, C., Jroundi, F., Vikman, M., 2018. Comparison of three DNA-extraction methods for MX-80 bentonite. MIND Project annual meeting 2018. Lausanne, May 7-9. 2018. Poster. Available online. http://www.mind15.eu/wp-content/uploads/2018/06/MIND_Abstract_2018_webb-1.pdf (accessed on September 7th, 2021).

Miettinen, H., Bomberg, M., Nyyssönen, M., Reunamo, A., Jørgensen, K.S., Vikman, M., 2019. Oil degradation potential of microbial communities in water and sediment of Baltic Sea coastal area. PLoS One 14, e0218834. https://doi.org/10.1371/journal.pone.0218834.

Miettinen, H., Bomberg, M., Le, T.M.K., Kinnunen, P., 2021. Identification and metabolism of naturally prevailing microorganisms in zinc and copper mineral processing. Minerals 11, 156. https://doi.org/10.3390/min11020156.

Moore, D., Reynolds, R., 1997. X-Ray Diffraction and the Identification and Analysis of Clay Minerals, 2nd edition. Oxford University Press, New York.

Nazina, T.N., Kosareva, I.M., Petrunyaka, V.V., Savushikina, M.K., Kudriavtsev, E.G., Lebedev, V.A., Ahunov, V.D., Revenko, Y.A., Khafizov, R.R., Osipov, G.A., Belyaev, S.S., Ivanov, M.V., 2004. Microbiology of formation waters from the deep repository of liquid radioactive wastes Severnyi. FEMS Microbiol. Ecol. 49, 97–107. https://doi.org/10.1016/j.femsec.2004.02.017.

Nilsson, R.H., Larsson, K.H., Taylor, A.F.S., Bengtsson-Palme, J., Jeppesen, T.S., Schigel, D., Kennedy, P., Picard, K., Glöckner, F.O., Tedersoo, L., Saar, I., Kõljalg, U., Abarenkov, K., 2019. UNITE database for molecular identification of fungi: Handling dark taxa and parallel taxonomic classifications. Nucleic Acids Res. 47, D259–D264. https://doi.org/10.1093/nar/gky1022.

OECD, 2000. Geological disposal of radioactive waste. Review of developments in the last decade. Downloadable from. https://www.oecd-nea.org/jcms/pl_13324/geological-disposal-of-radioactive-waste?details=true (accessed on September 7th, 2021).

Oren, A., 2014. The Family *Methanosarcinaceae*. In: Rosenberg, E., DeLong, E.F., Lory, S., Stackebrandt, E., Thompson, F. (Eds.), The Prokaryotes. Springer, Berlin, Heidelberg. https://doi.org/10.1007/978-3-642-38954-2_408.

Pedersen, K., 2010. Analysis of copper corrosion in compacted bentonite clay as a function of clay density and growth conditions for sulfate-reducing bacteria. J. Appl. Microbiol. 108, 1094–1104. https://doi.org/10.1111/j.1365-2672.2009.04629.x.

Pedersen, K., Bengtsson, A., Blom, A., Johansson, L., Taborowski, T., 2017. Mobility and reactivity of sulphide in bentonite clays – implication for engineered bentonite barriers in geological repositories for radioactive wastes. Appl. Clay Sci. 146, 495–502. https://doi.org/10.1016/j.clay.2017.07.003.

Pentráková, L., Su, K., Pentraák, M., Stucki, J.W., 2013. A review of microbial redox interactions with structural Fe in clay minerals. Clay Miner. 48, 543–560. https://doi.org/10.1180/claymin.2013.048.3.10.

Povedano-Priego, C., Jroundi, F., Lopez-Fernandez, M., Shrestha, R., Spanek, R., Martín-Sánchez, I., Villar, M.V., Ševců, A., Dopson, M., Merroun, M.L., 2021. Deciphering indigenous bacteria in compacted bentonite through a novel and efficient DNA extraction method: Insights into biogeochemical processes within the Deep Geological Disposal of nuclear waste concept. J. Hazard. Mater. 408, 124600 https://doi.org/10.1016/j.jhazmat.2020.124600.

Pruesse, E., Quast, C., Knittel, K., Fuchs, B.M., Ludwig, W., Peplies, J., Glöckner, F.O., 2007. SILVA: a Comprehensive online resource for quality Ccecked and aligned ribosomal RNA sequence data compatible with ARB. Nucleic Acids Res. 35, 7188–7196. https://doi.org/10.1093/nar/gkm864.

Pusch, R., Knutsson, S., Al-Taie, L., Hatem Mohammed, M., 2012. Optimal ways of disposal of highly radioactive waste. Nat. Sci. 4, 906–918. https://doi.org/10.4236/ns.2012.431118.

Qiu, Y.L., Sekiguchi, Y., Imachi, H., Kamagata, Y., Tseng, I.-C., Cheng, S.-S., Ohashi, A., Harada, H., 2003. *Sporotomaculum syntrophicum* sp. nov., a novel anaerobic, syntrophic benzoate-degrading bacterium isolated from methanogenic sludge treating wastewater from terephthalate manufacturing. Arch. Microbiol. 179, 242–249. https://doi.org/10.1007/s00203-003-0521-z.

Quast, C., Pruesse, E., Yilmaz, P., Gerken, J., Schweer, T., Yarza, P., Peplies, J., Glöckner, F.O., 2013. The SILVA ribosomal RNA gene database project: improved data processing and web-based tools. Nucleic Acids Res. 41, D590–D596. https://doi.org/10.1093/nar/gks1219.

Rajala, P., Carpén, L., Vepsäläinen, M., Raulio, M., Sohlberg, E., Bomberg, M., 2015. Microbially induced corrosion of carbon steel in deep groundwater environment. Front. Microbiol. 6, 647. https://doi.org/10.3389/fmicb.2015.00647.

Ribeiro, F.R., Fabris, J.D., Kostka, J.E., Komadel, P., Stucki, J.W., 2009. Comparisons of structural iron reduction in smectites by bacteria and dithionite: II. A variable-temperature Mössbauer spectroscopic study of Garfield nontronite. Pure Appl. Chem. 81, 1499–1509. https://doi.org/10.1351/PAC-CON-08-11-16.

Schloss, P.D., Westcott, S.L., Ryabin, T., Hall, J.R., Hartmann, M., Hollister, E.B., Lesniewski, R.A., Oakley, B.B., Parks, D.H., Robinson, C.J., Sahl, J.W., Stres, B., Thallinger, G.G., Van Horn, D.J., Weber, C.F., 2009. Introducing Mothur: open-source, platform-independent, community-supported software for de- scribing and comparing microbial communities. Appl. Environ. Microbiol. 75, 7537–7541. https://doi.org/10.1128/AEM.01541-09.

Schwartz, E., Fritsch, J., Friedrich, B., 2013. H_2-metabolizing prokaryotes. In: Rosenberg, E., DeLong, E.F., Lory, S., Stackebrandt, E., Thompson, F. (Eds.), The Prokaryotes. Springer, Berlin, Heidelberg. https://doi.org/10.1007/978-3-642-30141-4_65.

Sellin, P., Leupin, O.X., 2013. The use of clay as an engineered barrier in radioactive-waste management – a review. Clay Clay Miner. 61, 477–498. https://doi.org/10.1346/CCMN.2013.0610601.

Sohlberg, A., Bomberg, M., Miettinen, H., Salavirta, H., Vikman, M., Itävaara, M., 2015. Revealing the unexplored fungal communities in deep groundwater of crystalline

bedrock fracture zones in Olkiluoto, Finland. Front. Microbiol. 6, 573. https://doi.org/10.3389/fmicb.2015.00573.

Spring, S., Rosenzweig, F., 2006. The Genera *Desulfitobacterium* and *Desulfosporosinus*: Taxonomy. In: Dworkin, M., Falkow, S., Rosenberg, E., Schleifer, K.H., Stackebrandt, E. (Eds.), The Prokaryotes. Springer, New York, NY. https://doi.org/10.1007/0-387-30744-3_24.

Stroes-Gascoyne, S., Hamon, C.J., Maak, P., 2011. Limits to the use of highly compacted bentonite as a deterrent for microbiologically influenced corrosion in a nuclear fuel waste repository. Phys. Chem. Earth 36, 1630–1638. https://doi.org/10.1016/j.pce.2011.07.085.

Stucki, J.W., Kostka, J.E., 2006. Microbial reduction of iron in smectite. C.R. Geoscience. 338, 468–475. https://doi.org/10.1016/j.crte.2006.04.010.

Stucki, J.W., Lee, K., Zhang, L., Larson, R.A., 2002. Effects of iron oxidation state on the surface and structural properties of smectites. Pure Appl. Chem. 74, 2081–2094. https://doi.org/10.1351/pac200274112145.

Umezawa, K., Watanabe, T., Miura, A., Kojima, H., Fukui, M., 2016. The complete genome sequences of sulfur-oxidizing *Gammaproteobacteria Sulfurifustis variabilis* skN76^{T} and *Sulfuricaulis limicola* HA5^{T}. Stand. Genomic Sci. 11, 71. https://doi.org/10.1186/s40793-016-0196-0.

Vikman, M., Matusewicz, M., Sohlberg, E., Miettinen, H., Tiljander, M., Järvinen, J., Itälä, A., Rajala, P., Raulio, M., Itävaara, M., Muurinen, A., Olin, M., 2018. Long-term experiment with compacted bentonite. VTT Technology 332. Downloadable from. https://cris.vtt.fi/files/19390120/T332.pdf (accessed on September 7th, 2021).

Wagner, M., Roger, A.J., Flax, J.L., Brusseau, G.A., Stahl, D.A., 1998. Phylogeny of dissimilatory sulfite reductases supports an early origin of sulfate respiration. J. Bacteriol. 180, 2975–2982. https://doi.org/10.1128/JB.180.11.2975-2982.1998.

Watanabe, M., Kojima, H., Fukui, M., 2018. Review of *Desulfotomaculum* species and proposal of the genera *Desulfallas* gen. Nov., *Desulfofundulus* gen. Nov., *Desulfofarcimen* gen. Nov. and *Desulfohalotomaculum* gen. Nov. Int. J. Syst. Evol. Microbiol. 68, 2891–2899. https://doi.org/10.1099/ijsem.0.002915.

Wrighton, K., Agbo, P., Warnecke, F., Weber, K.A., Brodie, A.L., DeSAntis, T.Z., Hugenholtz, P., Andersen, G.L., Coates, J.D., 2008. A novel ecological role of the Firmicutes identified in thermophilic microbial fuel cells. ISME J. 2, 1146–1156. https://doi.org/10.1038/ismej.2008.48.

Wu, X., Holmfeldt, K., Hubalek, V., Lundin, D., Åström, M., Bertilsson, S., Dopson, M., 2016. Microbial metagenomes from three aquifers in the Fennoscandian shield terrestrial deep biosphere reveal metabolic partitioning among populations. ISME J. 10, 1192–1203. https://doi.org/10.1038/ismej.2015.185.

Zavarzina, D.G., Sokolova, T.G., Tourova, T.P., Chernyh, N.A., Kostrikina, N.A., Bonch-Osmolovskaya, E.A., 2007. *Thermincola ferriacetica* sp. nov., a new anaerobic, thermophilic, facultatively chemolithoautotrophic bacterium capable of dissimilatory Fe(III) reduction. Extremophiles. 11, 1–7. https://doi.org/10.1007/s00792-006-0004-7.

Zhou, Z., Pan, J., Wang, F., Gu, J.-D., Li, M., 2018. Bathyarchaeota: globally distributed metabolic generalists in anoxic environments. FEMS Microbiol. Rev. 42, 639–655. https://doi.org/10.1093/femsre/fuy023.